Honours Thesis:
Modeling ultrashort laser pulses interacting with molecules through the Maxwell-Schrödinger coupling, gauge theory and numerical analysis

Reynaldo J. Arteaga
Supervisor: Emmanuel Lorin
Second Reader: Dave Amundsen

May 10, 2012

Preface

This paper illustrates a portion of the design of modeling ultrashort laser pulses through a dense gaseous media. It has many applications in the field of optics and particle chemistry. The emphasis of this paper is to illustrate the theory of gauges and how it plays a role in the model. Moreover, we demonstrate the numerical analysis on the velocity gauge, and the gauge transformations from the velocity to length one. The outcome of this paper is a broad overview of the model accomplished through collecting relevant information from various papers in order for the reader to comprehend the model before stepping into more detailed papers on the topic.

Acknowledgements

I would like to thank all my family and friends who helped me reach to this point. I would like to give a special thanks to Emmanuel Lorin, who was the supervisor and mentor throughout this process. Without his help, this paper would never have existed.

Contents

1 Introduction

1.1 Real Life Application and Model

Light Amplification by Stimulated Emission of Radiation commonly known as a laser has developed substantially over the past 50 years. Lasers that have a pulse time duration less than 1 *picosecond* $(10^{-12}s)$ are commonly known as ultrashort laser pulses. In order to further comprehend the instrumental use of this laser technology, let us take a look at some numerical values of the Hydrogen atom. The period of circulation of an electron in the ground state is 24.6 *attoseconds* $(10^{-18}s)$. The electric field E and intensity I in that orbit are: $E = 5 \times 10^{11} V/m$ and $I = cE^2/8\pi = 3 \times 10^{16} W/cm^2$. Intense pulses of order $\leq 10^{-16}s$ can allow the control of the dynamics inside the molecule. Attosecond science involves studying dynamics at the scale of atoms and molecules. Its the science of electrons in atoms, molecules, and solids. In order to understand how molecules are bonded, or how the bonds change, we need a technology that allows us to image this on their time scale and space. Ultrashort and intense laser pulses are then an essential tool for attosecond science due to its ability of working at the molecular scale.
The main goal of this work is to introduce a model to study high order nonlinear phenomena such as Above Threshold Ionization (ATI), High Harmonics Generation (HHG), filamentation, etc. This is accomplished through intense laser pulses interacting with molecules. Other applications of the ultrashort laser pulses consist of controlled nuclear fusion by inertial confinement, quantum dynamic imaging and attosecond pulse generation. All these various potentials for the ultrashort laser pulses motivate the detailed study of this model.
Molecular behaviour excited by intense and ultrashort electric fields is modeled using a time-dependent laser-molecule Schrödinger equation (TDSE) with the Maxwell equations. The TDSE can be explicitly written in various equivalent forms as detailed in later chapters. A concept that brings rise to interchangeable or equivalent equations is the Lagrangian. The Lagrangian is a function that describes the dynamics of a system. In this framework, the system consists of particles and electric fields. Within the paper, we demonstrate that moving from one Lagrangian to another can be done through a unitary transformation. The Hamiltonian represents the sum of the kinetic energies and the potential energies of all the particles associated to the system. The Hamiltonian corresponds to the TDSE in our framework. Using the same unitary transformation applied for the change of Lagrangian, it is possible to go from one Hamiltonian to another under the new Lagrangian.

Furthermore, within a choice of Lagrangian, there exists multiple choices of Hamiltonians. This paper will focus on the selection of the Coulomb gauge. Within the framework of the Coulomb gauge, the two Hamiltonians that will be studied thoroughly in this paper are commonly referred as the velocity gauge and the length gauge.

This paper is organized as follows: Section 2 is devoted to the coupling of the Maxwell-Schrödinger equations used to model laser-gas interaction. Section 3 involves the equivalent Lagrangians and the gauges within each Lagrangian. Section 4 discusses the Coulomb, Lorentz and other gauge fields that can be selected when we fix a gauge. Section 5 adopts the Coulomb gauge field, and illustrates the comparison between the length gauge against the Coulomb gauge. Section 6 uses a finite difference scheme to approximate the TDSE under two gauges in which we study the stability, consistency and convergence. Section 7 explains the computing aspects behind the model, specifically the code that is implemented and the parallel computing that occurs behind the scenes. In Section 8 numerical simulations and design of the computing aspects is examined to demonstrate that the two gauges are fairly consistent. However, we will discuss why they do not produce the same numerical results even though theory tells us that they are equivalent.

2 Maxwell-Schrödinger

The coupling of the Maxwell and Schrödinger equations is how we propose to model laser pulses interacting with molecules. We will discuss this and how the Maxwell-Schrödinger equations are properly linked together and the motivation behind our choice of the model. There exists other models that are common in nonlinear optics, that will be discussed later in this chapter.

2.1 Global Description

The coupling of the Maxwell and Schrödinger equations can be decomposed into three main processes.

1. The first step consists of considering the TDSE. The interest of solving the TDSE is to acquire the solution ψ which can then be used in order to obtain the dipole moment. The dipole moment is computed in one-dimension as follows: $p(t) = \int_{\mathbb{R}} |\psi(x,t)|^2 x \, dx$, where ψ is the solution of the TDSE. The TDSE in general is written as :

$$\mathtt{i}\hbar\frac{\partial}{\partial t}\psi(x,t) = \hat{H}\psi(x,t), \;\; x \in \mathbb{R}, \;\; t > 0, \;\; \psi(x,0) = \psi_0(x),$$

   where ψ is the wavefunction, $\mathtt{i}$ is the imaginary unit, $\hbar$ is Planck's constant and $\hat{H}$ is the Hamiltonian operator. In later chapters we will examine distinct, equivalent TDSEs that can be used in this framework. We must be cautious since this portion is completed at the microscopic scale. With this set of solutions we move to the subsequent step of the coupling at the macroscopic level.

2. Discussed by Lorin, et al. in [8], the polarization term $\mathbf{P}$ can be expressed under the dipole approximation as: $\mathbf{P}(r,t) = \mathcal{N}(r)\sum_{i=1}^{m}\mathbf{P}_i(r,t)$ where $\mathcal{N}(r)$ is the molecular density dependent on the gas which the laser is interacting with. The explicit formulation of $\mathbf{P}(r,t)$ is discussed later in the paper (2.2). The solution $\psi(x,t)$ physically represents the dipole moment. This step now works at the macroscopic level by using the numerous solutions of the TDSEs that were computed earlier. The relevance of finding the polarization comes from the response of the gas acting on the electromagnetic field. This leads to the final step of the model.

3. Lastly, we use the computed polarization $\mathbf{P}$ in order to solve the Maxwell equations. At the macroscopic level we solve the system for

one molecule in the gas using the polarization. All the TDSEs that were previously solved result into one molecule at the microscopic level. The solution of the Maxwell equations gives us the updated electric and magnetic field which we then use as the initial data for the TDSEs.

As described by Lorin et al. [8], mathematically we consider the coupling of the three-dimensional macroscopic Maxwell equations with many TDSEs. We will work under the dipole approximation, so that the electric field will be constant at the molecular scale. This is valid when the smallest internal wavelengths $\lambda_{\min}$ of the electromagnetic field are much larger than the molecule size ℓ, that is $\ell = o(\lambda_{\min})$. The molecular density is supposed to be constant in time and is given by $\mathcal{N} \in C_0^\infty(\Omega)$ where $r = (x, y, z)^T$ the space variable in $\Omega \subset \mathbb{R}^3$

$$\left\{\begin{array}{lcl} \partial_t \mathbf{B}(\mathbf{r},t) & = & -c\nabla \times \mathbf{E}(\mathbf{r},t) \\ \partial_t \mathbf{E}(\mathbf{r},t) & = & c\nabla \times \mathbf{B}(\mathbf{r},t) - 4\pi \partial_t \mathbf{P}(\mathbf{r},t) \\ \nabla \cdot \mathbf{B}(\mathbf{r},t) & = & 0 \\ \nabla \cdot \big(\mathbf{E}(\mathbf{r},t) + 4\pi \mathbf{P}(\mathbf{r},t)\big) & = & 0 \end{array}\right. \tag{2.1}$$

with

$$\left\{\begin{array}{lcl} \mathbf{P}(\mathbf{r},t) = \mathcal{N}(\mathbf{r}) \sum_{i=1}^m \mathbf{P}_i(\mathbf{r},t) & = & \mathcal{N}(\mathbf{r}) \sum_{i=1}^m \chi_{\Omega_i}(\mathbf{r}) \int_{R^3 \times R_+} \psi_i(R',\mathbf{r}',t)\mathbf{r}'\psi_i^*(R',\mathbf{r}',t) d\mathbf{r}' dR' \\ \mathtt{i}\partial_t \psi_i(R',\mathbf{r}',t) & = & -\dfrac{\triangle_{\mathbf{r}'}}{2}\psi_i(R',\mathbf{r}',t) - \dfrac{\triangle_{R'}}{m_p}\psi_i(R',\mathbf{r}',t) \\ & + & \theta(R',\mathbf{r}') \cdot \mathbf{E}_{\mathbf{r}_i}\psi_i(R',\mathbf{r}',t) \\ & + & \Big(V_i(R') + V_c(R',\mathbf{r}')\Big)\psi_i(R',\mathbf{r}',t), \qquad \forall i \in \{1,...,m\}. \end{array}\right. \tag{2.2}$$

In (2.2), V_c denotes the Coulomb potential, V_i the nucleus potential and θ is a regular vector function with compact support $\mathcal{D}_1$ equal to $\mathbf{r}'$ on a compact set $\mathcal{D}_2 \subset \mathcal{D}_1$. In the case of a H_2^+-molecule gas, where the 3-body problem is transformed by symmetry into a 2-body problems the potentials write

$$V_c(R',\mathbf{r}') = -\frac{1}{\sqrt{x'^2 + (y' - R'/2)^2 + z'^2}} - \frac{1}{\sqrt{x'^2 + (y' + R'/2)^2 + z'^2}}, V_i(R') = \frac{1}{R'} \tag{2.3}$$

Ω_i denotes the macroscopic spatial domain containing a molecule of reference of wavefunction ψ_i, and $\mathbf{P}_i$ denotes the macroscopic polarization associated

to this domain. The space Ω_i contains $\mathcal{N}(\mathbf{r})\text{vol}(\Omega_i)$ molecules represented by ψ_i. Naturally we have $\cup_{i=1}^{m}\Omega_i = \Omega$.
Functions χ_{Ω_i} are defined by $\chi \otimes \mathbf{1}_{\Omega_i}$ where $\chi \in \mathcal{C}_0^\infty(\mathbb{R}^3)$ is a plateau function and $\mathbf{1}_{\Omega_i}$ is the characteristic function of Ω_i. Finally $\mathbf{E}_{\mathbf{r}_i}$ denotes the electric field (supposed constant in space) in Ω_i. In the following we will denote $\bar{\psi} = (\psi_1, ..., \psi_m)^T$.
The solution we obtain is in the form of the magnetic field $\mathbf{B}$ and electric field $\mathbf{E}$. In this paper, we consider the one-dimensional case so the magnetic field $\mathbf{B}$ is equal to $\mathbf{0}$. However, the point of interest in this paper is the comparison between equivalent TDSEs and their corresponding dipole moments.
In the case where the laser is passing through vacuum and there is no interaction with any molecule, this corresponds to the polarization being equal to $\mathbf{0}$. In this situation there is no need for the first two stages, i.e. there is no point in solving the TDSEs and computing the polarization since it is $\mathbf{0}$.

2.2 Macroscopic and Microscopic Grid

The models solution is obtained from our Maxwell-Schrödinger coupled equations. Within the framework of this paper, the two main choices of TDSEs are commonly known as the length gauge and velocity gauge. Their explicit equations will be discussed thoroughly in later chapters. The Maxwell equations are written at a macroscopic level while the Schrödinger equation is at the microscopic level. With these two different scales in mind, we solve our system in the one-dimensional case in the following order:

1. Partition the entire domain into $N \in \mathbb{N}$, subdomains.
2. In the current subdomain solve $N_S \in \mathbb{N}$, TDSE's.
3. Compute the polarization using the solutions to the N_S TDSE's
4. Solve one set of Maxwell equations using the polarization computed in step 3.
5. Use the solution of the Maxwell equations (electric and magnetic field) as the initial data for the TDSE's in the next subdomain.
6. Repeat steps 2 through 5 a total of N times.

The three stages listed above is the numerical approach to the former three steps in the previous section (2.1). The steps proposed in section (2.2) is how we properly couple the Maxwell-Schrödinger equations in order to model laser-gas interaction.

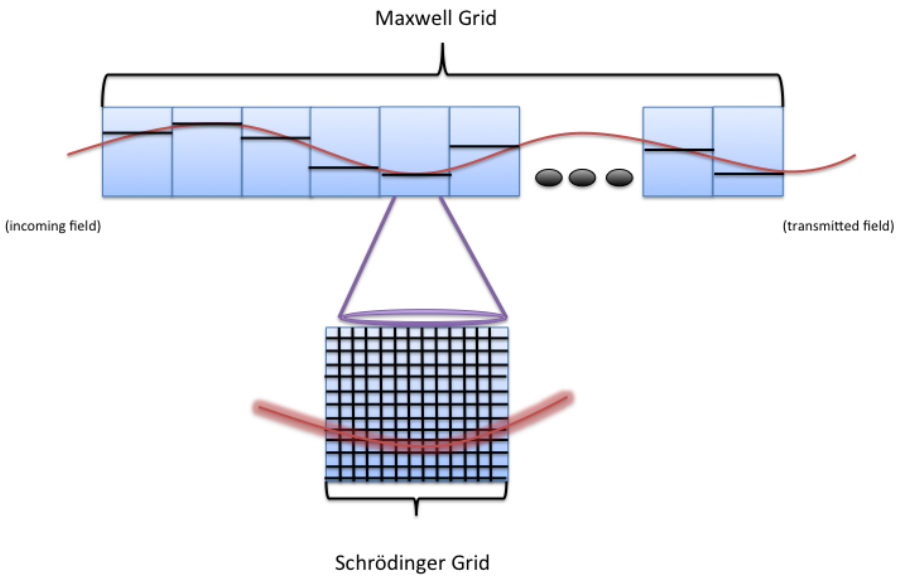

Figure 1: Macroscopic-Maxwell and microscopic-Schrödinger grid in the one-dimensional case with an incoming pulse.

2.3 Harmonics

Within this paper, there are three main components that revolve around the concept of the harmonics spectrum:

1. The dipole moment in one-dimension is defined as : $p(t) = \int_{\mathbb{R}} |\psi(x,t)|^2 x \, dx$.
2. The harmonic spectrum of the dipole moment is defined as: $\left(\omega, \ |\hat{p}(\omega)|^2\right)$.
3. The harmonic spectrum of the electric field is defined as: $\left(\omega, \ |\hat{\mathbf{E}}(\omega)|^2\right)$.

where ω is the incoming pulse and the $\hat{}$ operator represents the Fourier Transform. In the one-dimensional case, the polarization is equal to the molecular density times the dipole moment:

$$\mathbf{P}(x,t) = \mathcal{N}(x) \int_{\mathbb{R}} |\psi(x,t)|^2 x \, dx.$$

For this reason we compute the dipole moment and are interested in its solution.
The orders of the harmonics correspond to the odd multiples of ω_0, where the incoming pulse has a frequency of ω_0. Most nonlinear optics models neglect the harmonics and nonlinearities beyond the third one (Kerr effect), whereas we compute N_c-orders ($N_c \in \mathbb{N}$ and $N_c\omega_0$ represents a cutoff frequency). This is a consequence of the model being able to adapt to ultrashort laser pulses where the harmonics after ω_0 are not negligible. Conjecture 1 [8] illustrates that the electric field spectrum possesses a plateau (High Order Harmonic Generation) then a cut-off frequency, beyond which the harmonics are negligible. Corkum [8] conjectures that there exists an integer N_c such that the cut-off frequency is located around: $N_c\omega_0 \approx 3.17U_p + I_p$ where ω_0 is the frequency of the incoming pulse, I_p is the ionization potential of the atom/molecule, $U_p = e^2|\mathbf{E}_0|^2/4m\omega_0^2$ is the pondermotive energy of an electron in an oscillatory field $\mathbf{E}(t) = \mathbf{E}_0\cos(\omega_0 t)$ of maximum intensity $e\mathbf{E}_0^2/8\pi$. The important idea for this paper is that there exists a cut-off frequency since we have no necessity in this approximate value.

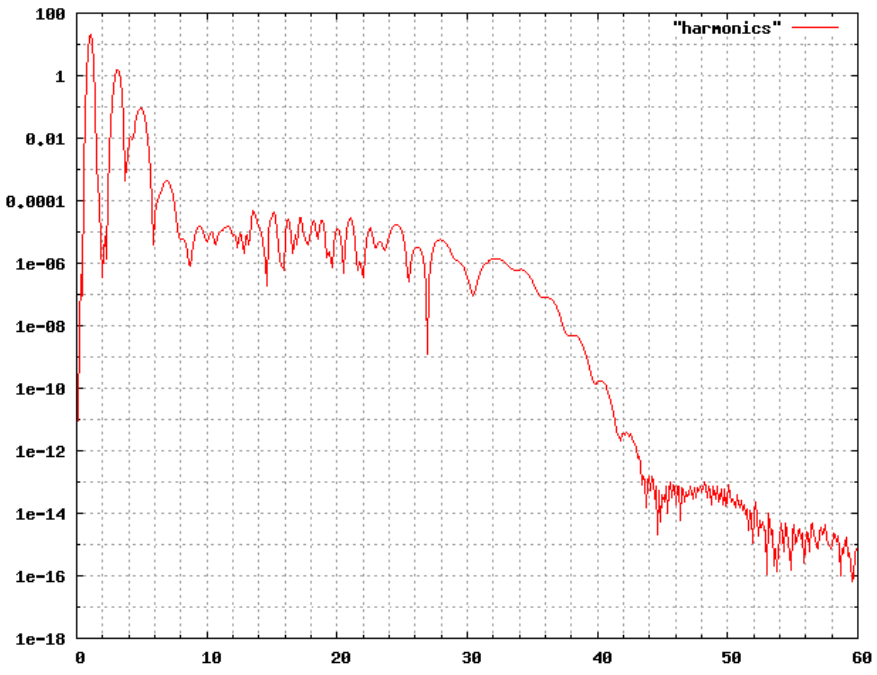

Figure 2: Harmonics spectrum of the dipole moment

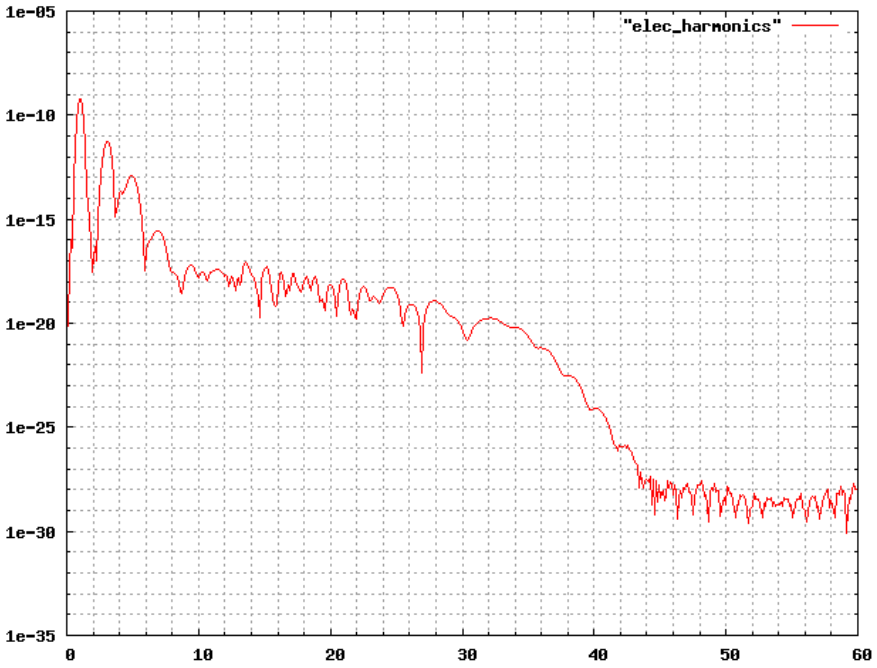

Figure 3: Harmonics spectrum of the electric field

2.4 Motivation

Although the coupling of the Maxwell and Schrödinger equations is not the only existing approach for modelling lasers interacting with molecules, it is more precise to the current models for some extreme regimes. The current models developed in nonlinear optics involve applying several approximations evolved from perturbation theory to the Maxwell and TDSE's in order to arrive at the nonlinear Maxwell and nonlinear Schrödinger equations. Within these approximations includes the fact that the amplitude of the incoming electric field, $|\mathbf{E}_0| \ll 1$ which facilitates perturbation methods. Although the nonlinear optics model does hold true under their assumptions, there is much more restriction on the possiblities of the choice of laser pulse. Specifically, their model can not account for ultrashort and intense laser pulses, whereas the Maxwell-Schrödinger equations are able to model it very well.

Moreover, due to this assumption of the amplitude of the incoming electric field (i.e. laser), $|\mathbf{E}_0| \ll 1$, macroscopic nonlinear optics models neglect all

the harmonics and nonlinearities beyond the third harmonic. The justification for this choice is because only the first three harmonics ω_0, $3\omega_0$ and $5\omega_0$ are very prominent and the rest of the harmonics to follow are negligible and can be ignored. Whereas when we work with ultrashort and intense laser pulses, the higher order harmonics are no longer neglible.

2.5 Existence and Uniqueness

In order for our model to be well-posed, we must ensure that there exists a solution and that it is unique. In [8] they detail the proof of existence and uniqueness. We denote by $(\mathbf{E}_0, \mathbf{B}_0, \bar{\psi}_0)^T$ the initial data of the system where $\bar{\psi}_0 = (\psi_{0,1}, ..., \psi_{0,m})^T$. We will first suppose that $\mathbf{E}_0$, $\mathbf{B}_0$ belong to $\big(H^1(\Omega)\big)^3$ and $\bar{\psi}_0 \in \big(H^1(\mathbb{R}^3 \times \mathbb{R}_+) \cap H_1(\mathbb{R}^3 \times \mathbb{R}_+)\big)^m$with the following definition.

$$\begin{aligned} H_1(\mathbb{R}^3 \times \mathbb{R}_+) &= \Big\{ u \in L^2(\mathbb{R}^3 \times \mathbb{R}_+), \|u\|_{H_1^+} \\ &= \int_{\mathbb{R}^3 \times \mathbb{R}_+} \big(1 + \|(R', \mathbf{r}')^T\|_2^2\big)|u(R', \mathbf{r}')|^2 dR' d\mathbf{r}' < \infty \Big\}. \end{aligned}$$

In the following we will respectively denote by L^2, H^1, H_1^+, the sets $L^2(\mathbb{R}^3 \times \mathbb{R}_+)$, $H^1(\mathbb{R}^3 \times \mathbb{R}_+)$, $H_1(\mathbb{R}^3 \times \mathbb{R}_+)$. We now justify the introduction of such a model by proving its well-posedness for a H_2^+ gas. Note that for other gas which corresponds to change the potentials (2.3), the analysis presented in the proof is *a priori* still valid, but may require additional technical but secondary difficulties.

Theorem 2.1. *Suppose that* $(\mathbf{E}_0, \mathbf{B}_0) \in \big(H^1(\Omega)\big)^3 \times \big(H^1(\Omega)\big)^3$, $\bar{\psi}_0 \in \big(H^1(\Omega) \cap H_1^+\big)^m$ *with* $\bar{\psi}(R' = 0, \mathbf{r}', t) = 0 \in R^m$ *for all* $\mathbf{r}' \in \mathbf{R}^3$ *and* $t \in R_+$ *and* $\mathcal{N} \in \mathcal{C}_0^\infty(\Omega)$. *Then there exists a time* $T > 0$ *for which there exists a unique* $(\mathbf{E}, \mathbf{B}, \bar{\psi}) \in \Big(L^\infty\big(0, T; (H^1(\Omega))^3\big) \times H^1\big(0, T; (L^2(\Omega))^3\big)\Big)^2 \times L^\infty\big(0, T; (H^1 \cap H_1^+)^m\big)$ *solution of (1) and (2).*

3 Mathematical Theory

Now that we have discussed the approach that the model takes, we will go into detail on the choice of the TDSE (or Hamiltonian). The invariance in the Maxwell equations and changing of Lagrangian that will lead to distinct, equivalent Hamiltonians are described precisely in this chapter. Lastly, the relation between the physical observables in different Hamiltonians will be studied.

3.1 Maxwell invariance

Let $\overrightarrow{\mathbf{j}}(r,t)$ be the current given by:

$$\partial_t \mathbf{j} + \frac{1}{\tau_c}\mathbf{j} = \frac{e^2}{m_e}\rho\mathbf{E},$$

where $e = m_e = 1$ in $a.u.$, τ_c is the collision time and $\mathbf{E}(r,t)$ is the electric field.
The Maxwell equations, in the three-dimensional and most general form are defined as the following set of equations [3] where $\mathbf{B}(r,t)$ is the magnetic field, $\rho(r,t)$ is the charge density, $r = (x,y,z)^T$

$$\begin{cases} \nabla \cdot \mathbf{E}(r,t) &= \dfrac{1}{\epsilon_0}\rho(r,t) \\ \nabla \cdot \mathbf{B}(r,t) &= 0 \\ \nabla \times \mathbf{E}(r,t) &= -\dfrac{\partial}{\partial t}\mathbf{B}(r,t) \\ \nabla \times \mathbf{B}(r,t) &= \dfrac{1}{c^2}\dfrac{\partial}{\partial t}\mathbf{E}(r,t) + \dfrac{1}{\epsilon_0 c^2}\mathbf{j}(r,t) \end{cases} \tag{3.1}$$

Due to the second and third Maxwell equations, there exists U, the scalar potential, and there exists $\mathbf{A}$ the vector potential such that we can rewrite $\mathbf{E}$ and $\mathbf{B}$ as:

$$\begin{cases} \mathbf{B}(r,t) &= \nabla \times \mathbf{A}(r,t), \\ \mathbf{E}(r,t) &= -\dfrac{\partial}{\partial t}\mathbf{A}(r,t) - \nabla U(r,t). \end{cases} \tag{3.2}$$

Now we use the following transformation which is commonly known as a gauge transformation:

$$\mathbf{A}(r,t) \mapsto \mathbf{A}'(r,t) = \mathbf{A}(r,t) + \nabla F(r,t), \tag{3.3}$$

$$U(r,t) \mapsto U'(r,t) = U(r,t) - \frac{\partial}{\partial t}F(r,t), \tag{3.4}$$

where F is an arbitrary differentiable function of r and t. This arbitrariness of the function F allows for the invariance in the gauges. A gauge refers to the redudant degrees of freedom in the Lagrangian [3]. The gauge transformation is used to transform a Hamiltonian into different gauges depending on the arbtirary differentiable function F. This possibility of describing the equations with various equivalent formulations leads us to the discussion of the Lagrangian and its respective Hamiltonians.

3.2 Lagrangian and Hamiltonian Formalism

The Lagrangian, L, is a function that describes the dynamics of a system. In [3]

> For a system having N degrees of freedom, giving the N generalized coordinates $x_1, \ldots, x_N$ and the corresponding velocities $x'_1, \ldots, x'_N$ at a given time completely determines the subsequent motion. The $2N$ quantities $x_1, \ldots, x_N$ and $x'_1, \ldots, x'_N$ form an ensemble of *dynamical variables*. The accelerations can be expressed at any time as a function of these variables. The resulting equations of motion are then second-order differential equations in time. The motion of the system is determined by integrating these equations.
>
> It is equally possible to specify the motion of the system by means of a variational principle. In the Lagrangian approach, one postulates the existence of a function $L(x_j, x'_j, t)$ called the *Lagrangian,* which depends on the coordinates and the velocities (and perhaps explicity on time), such that the integral of L between times t_1 and t_2 will be an extremum when $x_j(t)$ corresponds to the *real* path of the system between t_1 and t_2.
>
> $$S = \int_{t_1}^{t_2} L\left(x_j(t), x'_j(t), t\right) dt, \tag{3.5}$$
>
> where $j \in \{1 \ldots N\}$ and the S is the *action,* and the corresponding variational principle is called the principle of least action.

The Lagrangian is not unique and we will demonstrate in this chapter how to change from one to another along with the consequences of this change. The Hamiltonian, H, is defined as the sum of the kinetic energies and the potential energies of all the particles associated to the system. In this framework, the Hamiltonian is the operator that is embedded in the TDSE. Within

this paper we sometimes use the two terms TDSE and Hamiltonian interchangeably. The momentum conjugates to the velocity x_j are defined as:

$$\mathbf{p}_j = \frac{\partial L}{\partial x'_j}, j \in \{1 \dots N\}.$$

The Hamiltonian is related to the Lagrangian through the following equation:

$$H(x_j, p_j) = \sum_{j=1}^{N} x'_j \mathbf{p}_j - L. \tag{3.6}$$

3.3 Changing the Lagrangian

When we work with Lagrangians and gauge fields, we must decide which Lagrangian we wish to work under. Selecting a specific Lagrangian is a consequence of the realization that the Lagrangian is not unique for a dynamical system. In order to choose a specific Lagrangian, we often refer to this as making a choice of one gauge condition which fixes $\nabla \cdot \mathbf{A}$. By adding to the Lagrangian L, the time derivative of a function $F(x,t)$ (x and t are the space and time variable respectively) we arrive at a new Lagrangian:

$$L'(x_j, x'_j, t) = L(x_j, x'_j, t) + \frac{d}{dt}F(x_j, t), \quad j \in \{1 \dots N\}.$$

The action integral S' relative to L' is written using (3.5) as:

$$S' = \int_{t_1}^{t_2} L' dt = S + F(x_j(t_2), t_2) - F(x_j(t_1), t_1), \quad j \in \{1 \dots N\}.$$

L and L' are equivalent in regards to the momentum conjugate $\mathbf{p}_L$ with respect to the new Lagrangian is:

$$\mathbf{p}_{L'} = \frac{\partial L'}{\partial x'} = \frac{\partial L}{\partial x'} + \frac{\partial F}{\partial x} = \mathbf{p}_L + \frac{\partial F}{\partial x}.$$

Similarly to Lagrangian transformations, the Hamiltonians alteration illustrates a similar result:

$$\begin{aligned} H^{L'}(x, \mathbf{p}_{L'}) = x' \mathbf{p}_{L'} - L'(x_j, x'_j, t) &= x' \left(\mathbf{p}_L + \frac{\partial F}{\partial x} \right) - \left(L(x_j, x'_j, t) + x' \frac{\partial F}{\partial x} + \frac{\partial F}{\partial t} \right) \\ &= H^L(x, \mathbf{p}_L) - \frac{\partial F}{\partial t}, \end{aligned}$$

where $j \in \{1 \dots N\}$.

3.4 Lagrangian to Hamiltonian

By Applying Lagrange's equations to the momentum conjugates:

$$\frac{d}{dt}\left(\frac{\partial L}{\partial x_j'}\right) = \frac{\partial L}{\partial x_j}, j \in \{1 \dots N\}.$$

The time derivate of $\mathbf{p}_j$ is:

$$\mathbf{p}_j' = \frac{\partial L}{\partial x_j}.$$

As mentioned [3], this equation suggests the use of the coordinates and momenta as dynamical variables rather than the coordinates and velocities. We then substitute the Hamiltonian for the Lagrangian

$$H(x_j, \mathbf{p}_j) = \sum_{j=1}^{N} x_j' \mathbf{p}_j - L(x_j, x_j', t).$$

By differentiation we arrive at Hamilton's equations:

$$\begin{cases} x_j' &= \dfrac{\partial H}{\partial \mathbf{p}_j}, \\ x_j' &= -\dfrac{\partial H}{\partial x_j}. \end{cases}$$

There was previously N Lagrange second-order differential equations which have now been replaced by a system of $2N$ first-order differential equations. These $2N$ ordinary differential equations occur in the solving of the TDSE which will be discussed in detail in later chapters.

3.5 Unitary Transformation

A unitary transformation in general is a surjective linear transformation $T : V \to V$ satisfying,

$$\langle u, v \rangle = \langle Tu, Tv \rangle, \quad u, v \in V$$

where V is a complex vector space. Generalization of a gauge transformation corresponds to an unitary transformation. In order to move from Lagrangian to Lagrangian, and Hamiltonian to Hamiltonian, we apply a unitary transformation. A unitary transformation is written:

$$T(t) = \exp(\mathtt{i}\frac{q}{\hbar}F(x, x', \mathbf{A}, U, \mathbf{A}', U', t)),$$

and

$$\tilde{\psi} = T(t)\psi, \quad \tilde{G}(t) = T(t)G(t)T^{+}(t)$$

where q is the charge, $\hbar$ is Planck's constant, $\mathbf{A}$ is the vector potential, U is the scalar potential, x is the space coordinate, t is the time and $G(t)$ is the kinetic energy at time t.
Within one Lagrangian, we can define a new Hamiltonian $\tilde{H}$ as follows:

$$\tilde{H} = T(t)HT^{+}(t) + \mathtt{i}\hbar\frac{dT}{dt}T^{+}(t).$$

The unitary transformation is used to show that the transition amplitudes are equal for different Hamiltonians that will be discussed in section 5.4.

3.6 Physical Observables

Thus far we have exhibited the fact that we have equivalences between Lagrangians and Hamiltonians which allow us to transform one gauge to another. However we must also reflect on the physical observables and the consequences resulting from the gauge transformations.
The unitary transformation associated to the length and velocity gauge is

$$T(t) = \exp\left(-\frac{\mathtt{i}}{\hbar}qr \cdot \mathbf{A}(0,t)\right),$$

where q is the charge, $\hbar$ is Planck's constant, $r = (x, y, z)^T$, $\mathbf{A}(0,t)$ is the vector potential. We work with the dipole approximation where we assume the space variation of the electromagnetic field is negligible with respect to the molecule size.
Transition amplitude between two energy states (E_a, ϕ_a) to (E_b, ϕ_b) of $\tilde{H}_0$ (laser free Hamiltonian associated to $\tilde{H}$) is detailed here. When the gauge transformation is applied we then have

$$\tilde{H}_0\phi_{a,b} = E_{a,b}\phi_{a,b}.$$

Two possible cases to consider are:

1. The states ϕ_a and ϕ_b correspond to states of energy E_a and E_b for H_0 (laser free operator associated to H) as for $\tilde{H}_0$. The first particular case is $\mathbf{A}(0,t_0) = E(0,t_0) = \mathbf{A}(0,t_f) = E(0,t_f) = 0$ and $U(0,t_0) = U(0,t_f) = 0$, where t_0 and t_f are the initial (E_a, ϕ_a) and final (E_b, ϕ_b) times. ϕ represents the transition amplitude. This leads trivially to

   $$< \phi_a|U(t_f,t_0)|\phi_b > = < \phi_a|\tilde{U}(t_f,t_0)|\phi_b >,$$

   due to the fact that $T(t_0) = T(t_f) = 1$. U is the evolution operator.

2. In this case $\mathbf{A}(0,t) \neq 0$. ϕ_a and ϕ_b are states of ill-defined energies ($\neq E_a, E_b$)

$$H_0\phi_{a,b} \neq E_{a,b}\phi_{a,b}.$$

In that situation to study the transition from ϕ_a to ϕ_b, we remark first that

$$\psi(t_0) = T^+(t_0)\phi_a, \qquad \psi(t_f) = T^+(t_f)\phi_b$$

, so that the transition becomes:

$$< \psi(t_0)|U(t_f,t_0)|\psi(t_f) >= T(t_f)U(t_f,t_0)T^+(t_0)|\phi_b =< \phi_a|\tilde{U}(t_f,t_0)|\phi_b > .$$

In conclusion, we see that the transition amplitudes are equal.

4 Gauge Fixing

Gauges are a vital component to the model of ultrashort intense laser pulses, however the essence of its beauty are in the gauge transformations. They consist of transformations between possible gauges, forming a Lie group commonly referred to as the symmetry group or gauge group of the theory. Their relevance to the mathematical system is that in practice we can model the problem with various gauges which can be shown equivalent through unitary transformations. If the algorithms used are exact, we can achieve the exact same numerical results with different gauges. We are interested in this invariance because some gauges exhibit explicit variables that we wish to know. For example, the velocity gauge contains the electric potential of the system whereas after a gauge transformation the length gauge involves the electric field and no longer the electric potential. This brings rise to flexibility in which gauge we use, depending on the available data or preferred model. As we will detail further in the paper, every gauge has its strengths and weakenesses. Under exact mathematical methods all will result in the same solutions. There are factors that can make individual gauges much more efficient than their alternatives. This stimulates the curiosity of using several gauges under specific initial conditions.
All the gauges used for this problem have been adapted from the Coulomb Hamiltonian. The length and velocity gauges belong to the Coulomb Hamiltonian group of equivalent gauges. A picture illustrating the connections between the gauges and Hamiltonians on different levels is shown.

4.1 Coulomb Gauge

The Coulomb gauge is also known as the transverse gauge. It has the condition:

$$\nabla \cdot \mathbf{A} = 0$$

where $\mathbf{A}$ is the vector field. In this Coulomb gauge field, we have a set of gauges which can be shown to be equivalent through transformations. These include, length, velocity (or Coulomb), acceleration (or space translation). Consequence of the condition for the Coulomb gauge, along with the simplicity of the gauge field in comparison to the other possible fields, it is the most commonly used gauge involved in modeling this system.

4.2 Lorentz Gauge

The Lorentz gauge is defined by the gauge condition:

$$\nabla \cdot \mathbf{A}(r,t) + \frac{1}{c^2}\frac{\partial}{\partial t}U(r,t) = 0 \tag{4.1}$$

where $\mathbf{A}$ is the vector potential, U is the scalar potential, and c is the speed of light. The Lorentz gauge is the second most commonly used field for modeling the system. Covariant notation $\mathbf{A}^\mu$ for the potential four-vector takes on four values: $\mu = 1, 2, 3$ for spatial components and 0 for the time component. The contravariant components $\mathbf{A}^\mu$ with superscript index from the covariant components $\mathbf{A}_\mu$ where

$$\mathbf{A}_\mu = \sum_{v=1}^{N} g_{\mu\nu}\mathbf{A}^\mu$$

where $g_{\mu\nu}$ is the diagonal metric tensor ($g_{00} = +1,\ g_{11} = g_{22} = g_{33} = -1$,) stated by Cohen-Tannoudji et al. [3].
Similar to the Coulomb gauge, the Lorentz gauge has some common local gauges. The general expression of the Lagrangian for the Lorentz gauge is:

$$L = -\frac{1}{4}F_{\mu\nu}F^{\mu\nu} - \frac{1}{2\alpha}(\partial_\mu \mathbf{A}^\mu)^2 \tag{4.2}$$

Where $\alpha = 0,\ 1,\ -2$, is the Feynman, Landau, and Yennie & Fried gauge respectively.

4.3 Other Gauge Fields

Another gauge field is the Poincaré/Multipolar/Fock-Schwinger gauge. Whereas the Coulomb gauge has the condition $\nabla \cdot \mathbf{A} = 0$, in the Poincaré gauge, the condition is $\mathbf{A}'$(r) is everywhere orthogonal to $r = (x, y, z)^T$. The potentials in this gauge are defined as

$$\begin{aligned} \mathbf{A}'(r,t) &= \mathbf{A}(r,t) + \nabla F(r,t) \\ U'(r,t) &= U(r,t) - \tfrac{\partial}{\partial t}F(r,t) \end{aligned}$$

where $\mathbf{A}$ is the vector potential, U is the scalar potential, and F is an arbitrary differentiable function.
As well, the new Lagrangian for the Poincaré gauge reads:

$$L' = L - \frac{d}{dt}\left[\sum_{\alpha=1}^{N} q_\alpha F(r_\alpha, t)\right] \tag{4.3}$$

Another very useful component to the Poincaré gauge is the fact that the potentials can be expressed easily as a function of the magnetic field $\mathbf{B}$ and the electric field $\mathbf{E}$.

$$\begin{aligned} \mathbf{A}'(r) &= -\int_0^1 u\, du\, \mathbf{r} \times \mathbf{B}(ru) \\ U'(r) &= -\int_0^1 du\, \mathbf{r} \cdot \mathbf{E}(ru) \end{aligned}$$

The dot product appears for U and the cross product for A since they are scalar and vector potentials respectively. Lastly, the Temporal or Hamiltonian gauge is another possible choice. It's driving component is that the scalar potential is zero.

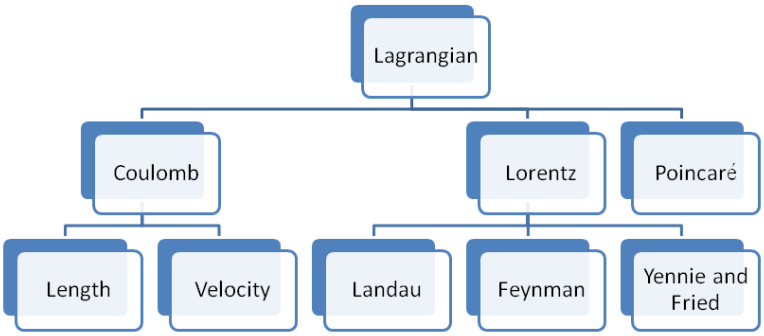

Figure 4: Gauge field hierarchy which develops from the Lagrangian. The relationship between sister nodes in the tree is that they are equivalent to one another.

5 Coulomb Gauge Field

The model that is proposed in this paper involves the choice of Lagrangian to be the Coulomb gauge field. Here we will study the possible Hamiltonians that can be derived from this Lagrangian. We will illustrate the unitary transformation that demonstrates the equivalence between Hamiltonians. Moreover, we will describe motivations for selecting one of these Hamiltonians. The Coulomb gauge is governed by the gauge condition that $\nabla \cdot \mathbf{A} = 0$

5.1 Velocity or Coulomb

Known by several names such as velocity, coulomb or radiation-field gauge; the TDSE for a 2 nucleus molecule can be expressed in the following equation in one-dimesion:

$$\mathtt{i}\partial_t \psi(x,t) = \left[-\frac{1}{2m}\Delta_x + V_c(x, R_0) - \frac{\mathtt{i}}{c}\mathbf{A}(t) \cdot \nabla_x + \frac{\|\mathbf{A}(t)\|^2}{2c^2} \right] \psi(x,t) \quad (5.1)$$

where $\mathbf{A}(t)$ denotes the electric potential, Δ_x is the kinetic operator, V_c is the electron-nucleus potential, x represents the electron position in the nucleus center of mass coordinates, c is the speed of light, R_0 is the internucleus distance supposed fixed because of the Born-Oppenheimer approximation. The velocity gauge is taken in Eulerian coordinates where the molecule-field interaction appears as a convenction term.
The Hamiltonian describing this velocity gauge, H^v, for a single-particle interacting with the field is [2]:

$$H^v(t) = -\frac{1}{2m}\Delta_x + V_c(x, R_0) - \frac{\mathtt{i}}{c}\mathbf{A}(t) \cdot \nabla_x + \frac{\|\mathbf{A}(t)\|^2}{2c^2}$$

where m is the mass, $\mathbf{A}(t)$ is the electric potential, $V_c(x)$ is the Coulomb potential.
If we extend this equation to a multicharge system, we obtain the following Hamiltonian [1],

$$H^v(t) = \sum_{k=1}^{N} \frac{1}{2m_k} \left(\mathbf{p}_k - q_k \mathbf{A}(t) \right)^2 + V_c(x_k)$$

where $\mathbf{p}_k$ is the momentum conjugate, q_k is the charge, $V_c(x_k)$ is the Coulomb potential and m_k is the mass, all at the k^{th} particle of the system.

5.1.1 Incompressible Flows

The appearance of the convection term has similarities with the convection-diffusion equations in fluid dynamics. The convection velocity is called the electromagnectic potential [2]

$$\mathbf{A}(t) = \int_0^t \mathbf{E}(s)ds.$$

Under this gauge, the $\nabla \cdot \mathbf{A} = 0$ is in a sense incompressible. The connection of the two equations has the possibility of applying methods from one field to help in solving the other. There are still some subtle but important differences between the two. We do not perform any rigorous analysis but we merely mention that there is a slight connection that could be taken further.

5.1.2 Transformation from Velocity to Length Gauge

The velocity gauge time dependent Schrödinger equation can be written as

$$\mathtt{i}\partial_t \psi(x,t) = \left[-\frac{1}{2}\Delta_x + V_c(x, R_0) - \frac{\mathtt{i}}{c}\mathbf{A}(t) \cdot \nabla_x + \frac{\|\mathbf{A}(t)\|^2}{2c^2} \right] \psi(x,t) \quad (5.2)$$

Proposition 1.1: The velocity TDSE is equivalent to the length gauge:

$$\mathtt{i}\partial_t \psi(x,t) = \left[-\frac{1}{2}\Delta_x + V_c(x, R_0) + x \cdot \mathbf{E}(t) \right] \psi(x,t) \quad (5.3)$$

with $\mathbf{E} = -\dfrac{\partial}{c\partial t}\mathbf{A}(t) \in L^\infty(\mathbb{R}_+)^3$ which denotes the electric field.

Proof: What is normally a classical result will be proved in more detail here.
The unitary transformation used is

$$\psi(x,t) \longmapsto \psi(x,t) \exp\left(-\frac{\mathtt{i}}{c^2} \int_0^t \|\mathbf{A}(s)\|^2 ds - \frac{\mathtt{i}}{c} x \cdot \mathbf{A}(t) \right) \quad (5.4)$$

Let us define:

$$\tau = -\frac{\mathtt{i}}{c^2} \int_0^t \|\mathbf{A}(s)\|^2 ds - \frac{\mathtt{i}}{c} x \cdot \mathbf{A}(t) \quad (5.5)$$

Now,

$$\begin{aligned}\partial_t\psi(x,t)e^{\tau} &= \psi_t(x,t)e^{\tau} + \tau_t\psi(x,t)e^{\tau} \\ &= [\psi_t(x,t) + \tau_t\psi(x,t)]e^{\tau} \\ &= \left[\psi_t(x,t) + \left(-\frac{\mathtt{i}}{c^2}\|\mathbf{A}(t)\|^2 - \frac{\mathtt{i}}{c}x\frac{\partial}{\partial t}\mathbf{A}(t)\right)\psi(x,t)\right]e^{\tau}\end{aligned}$$

$$\mathtt{i}\partial_t\psi(x,t)e^{\tau} = \left[\mathtt{i}\partial_t\psi(x,t) + \left(\frac{\|\mathbf{A}(t)\|^2}{c^2} + \frac{x}{c}\frac{\partial}{\partial t}\mathbf{A}(t)\right)\psi(x,t)\right]e^{\tau}. \qquad (5.6)$$

Then

$$\begin{aligned}\nabla_x\psi(x,t)e^{\tau} &= \nabla_x\psi(x,t)e^{\tau} + \psi(x,t)(\nabla_x\tau)e^{\tau} \\ &= \left[\nabla_x\psi(x,t) - \frac{\mathtt{i}}{c}\mathbf{A}(t)\psi(x,t)\right]e^{\tau}\end{aligned}$$

$$\begin{aligned}\Delta_x\psi(x,t)e^{\tau} &= (\Delta_x\psi(x,t) - \frac{\mathtt{i}}{c}A(t)(\nabla_x\psi(x,t)))e^{\tau} + (\nabla_x\psi(x,t) - \frac{\mathtt{i}}{c}\mathbf{A}(t)\psi(x,t))e^{\tau}(-\frac{\mathtt{i}}{c}\mathbf{A}(t)) \\ &= e^{\tau}\left[\Delta_x\psi(x,t) - \frac{2\mathtt{i}}{c}\mathbf{A}(t)\nabla_x\psi(x,t) + \frac{\|\mathbf{A}(t)\|^2}{c^2}\psi(x,t)\right]\end{aligned}$$

Moreover,

$$-\frac{1}{2}\Delta_x\psi(x,t)e^{\tau} = e^{\tau}\left[-\frac{1}{2}\Delta_x\psi(x,t) + \frac{\mathtt{i}}{c}\mathbf{A}(t)\nabla_x\psi(x,t) + \frac{\|\mathbf{A}(t)\|^2}{2c^2}\psi(x,t)\right] \qquad (5.7)$$

Substituting equation (5.7) into the right hand side of equation (5.2) we obtain:

$$\begin{aligned}\mathtt{i}\partial_t\psi(x,t)e^{\tau} &= e^{\tau}\left[-\frac{1}{2}\Delta_x\psi(x,t) + \frac{\mathtt{i}}{c}\mathbf{A}(t)\nabla_x\psi(x,t) + \frac{\|\mathbf{A}(t)\|^2}{2c^2}\psi(x,t)\right] \\ &+ \psi(x,t)e^{\tau}\left[V_c(x,R_0) - \frac{\mathtt{i}}{c}\mathbf{A}(t)\nabla_x + \frac{\|\mathbf{A}(t)\|^2}{2c^2}\right] \qquad (5.8)\end{aligned}$$

Lastly, using $\mathtt{i}\partial_t\psi(x,t)$ we combine (5.6) = (5.8) and isolate $\mathtt{i}\partial_t\psi(x,t)$ to get:

$$
\begin{aligned}
\mathtt{i}\partial_t\psi(x,t) &= -\frac{1}{2}\Delta_x\psi(x,t) + \frac{\mathtt{i}}{c}\mathbf{A}(t)\nabla_x\psi(x,t) + \frac{\|\mathbf{A}(t)\|^2}{2c^2}\psi(x,t) + \psi(x,t)V_c(x,R_0) \\
&\quad - \frac{\mathtt{i}}{c}\mathbf{A}(t)\nabla_x\psi(x,t) + \frac{\|\mathbf{A}(t)\|^2}{2c^2}\psi(x,t) + x\cdot E(t)\psi(x,t) - \frac{\|\mathbf{A}\|^2(t)}{c^2}\psi(x,t) \\
&= \left[-\frac{1}{2}\Delta_x + V_c(x,R_0) + x\cdot\mathbf{E}(t)\right]\psi(x,t)
\end{aligned}
$$

5.2 Length or Electric-Field

The Length Gauge TDSE can be written in three-dimensional as follows:

$$
\begin{aligned}
\mathtt{i}\frac{\partial\psi(x,y,z,t)}{\partial t} &= -\frac{2m_p+1}{4m_p}\left[\frac{\partial^2}{\partial x^2} + \frac{\partial^2}{\partial x^2} + \frac{\partial^2}{\partial z^2}\right]\psi(x,y,z,t) \\
&\quad - \frac{\psi(x,y,z,t)}{\sqrt{x^2+y^2+(z\pm R_0/2)^2}} \\
&\quad + \frac{2m_p+2}{2m_p+1}z\mathbf{E}(t)\cos(\omega t)\psi(x,y,z,t)
\end{aligned} \tag{5.9}
$$

where,

$$
\begin{aligned}
V_c &= -\frac{\psi(x,y,z,t)}{\sqrt{x^2+y^2+(z\pm R_0/2)^2}}, \\
r &= (x,y,z)^T, \\
\Delta_r &= \frac{\partial^2}{\partial x^2} + \frac{\partial^2}{\partial x^2} + \frac{\partial^2}{\partial z^2}, \\
c^2 &= \frac{2m_p}{2m_p+1}.
\end{aligned}
$$

Hence, we can rewrite the length gauge in a more compact form in the one-dimensional case:

$$
\mathtt{i}\partial_t\psi(x,t) = \left[-\frac{1}{2}\Delta_x + V_c(x,R_0) + x\mathbf{E}(t)\right]\psi(x,t) \tag{5.10}
$$

where $\mathbf{E}$ represents the electric field, V_c is the electron-nucleus potential, x represents the electron position in the nucleus center of mass coordinates, R_0 is the internucleus distance which is supposed fixed because of the Born-Oppenheimer approximation [7].

The length gauge is taken in Eulerian coordinates where the molecule-field interaction appears as a potential term.
The Hamiltonian that describes the length gauge, $H^l(t)$, can be written for a single-particle interacting with a field as [2]:

$$H^l(t) = -\frac{1}{2}\Delta_x + V_c(x, R_0) + x\mathbf{E}(t).$$

Extending this equation into a multicharge system we obtain [1]:

$$H^l(t) = \sum_{k=1}^{N} \frac{1}{2m_k}{\mathbf{p}_k}^2 + V_c(x_k) - x_k \cdot \mathbf{E}(t),$$

where $\mathbf{p}_k$ is the momentum conjugate, q_k is the charge, $V_c(x_k)$ is the Coulomb potential and m_k is the mass, all at the k^{th} particle of the system.

5.3 Space Translation or Acceleration

The acceleration or space translation TDSE can be written as follows:

$$\mathtt{i}\partial_t\psi(x,t) = \left[-\frac{1}{2m}\Delta_x - \frac{1}{\sqrt{x^2-\alpha(t)}}\right]\psi(x,t), \tag{5.11}$$

$$\alpha(t) = \frac{q}{m}\int_0^t dt'\mathbf{A}(t'), \tag{5.12}$$

where q is the charge, m is the mass, x is the space coordinate, and $\mathbf{A}(t')$ is the vector potential at time t'. The unitary transformation applied to the velocity gauge is known as the Kramers-Henneberger (kh) transformation [1]:

$$T_{kh}(t) = \exp\left\{\frac{\mathtt{i}q}{m\hbar}\mathbf{p}\cdot\int_0^t dt'\mathbf{A}(t')\right\}\exp\left\{-\frac{\mathtt{i}q^2}{2m\hbar}\int_0^t dt'\mathbf{A}^2(t')\right\}$$

where $\hbar = 1$.
The Hamiltonian that demonstrates the single-particle interacting with a field can be written as [2]:

$$H^{kh}(t) = \frac{\mathbf{p}^2}{2m} + V_c(x-\alpha(t))$$

The Hamiltonian illustrated by a multicharge system is shown as [1]:

$$H^{kh}(t) = \sum_{k=1}^{N}\frac{{\mathbf{p}_k}^2}{2m_k} + V_c\left(x_k - \frac{q_k}{m_k}\int_0^t dt'\mathbf{A}(t')\right).$$

where $\mathbf{p}_k$ is the momentum conjugate, q_k is the charge, $V_c(x_k)$ is the Coulomb potential and m_k is the mass, all at the k^{th} particle of the system.

5.3.1 Transformation from Velocity to Acceleration Gauge

We detail how to obtain the acceleration (or space translation) gauge from the velocity gauge. The acceleration gauge is performed in the Lagrangian (moving) coordinate system and is defined as:

$$\mathtt{i}\frac{\partial\psi(x,y,z,t)}{\partial t} = -\frac{2m_p+1}{4m_p}\left[\frac{\partial^2}{\partial x^2}+\frac{\partial^2}{\partial y^2}+\frac{\partial^2}{\partial z^2}\right]\psi(x,y,z,t) - \frac{\psi(x,y,z,t)}{\sqrt{x^2+y^2+(z-\alpha(t)\pm R/2)^2}}$$

where $\alpha(t)$ is given by (5.12). In order to arrive at the space translation gauge, we transform the velocity (Coulomb) gauge by changing the variable z by:

$$z \mapsto z + \frac{2m_p+1}{2m_p}\int_0^t\int_0^s \mathbf{E}(\tau)d\tau ds = z+\alpha(t).$$

The space translation method involves moving coordinates requiring adaptive grid methods to solve the equations. For large electron-nuclear separation which occurs in dissociative ionization processes, the grid moves in phase with the electron wavefunction making it exact.

5.4 Transition Amplitudes

Let us introduce two new representations (1) and (2) which are linked by a unitary transformation T. It can be proven [3] that in the general case, the transition matrices are theoretically identical, from a state ϕ_a to ϕ_b. Although identical in theory, from a perturbation point of view, some important differences may occur. As the length, velocity and acceleration gauges are related by a unitary transformation, their corresponding transition matrices are identical.
We consider a pulse $\mathbf{A}(0,t) = \mathbf{A}(t)\cos(\omega t)\mathbf{e}_x$ with $T\omega \gg 1$. We recall that the transition element from ϕ_a to ϕ_b is

$$S_{ab} = \lim_{t_2\to+\infty}\lim_{t_1\to-\infty} < \phi_a|U^{l,v,a}(t_2,t_1)|\phi_b >$$

where $U^{l,v,a}$ is the evolution operator for respectively length, velocity and acceleration gauges. It can be proven by a perturbation approach where the incoming pulse $\mathbf{A}_0 \ll 1$ that

- When passing through one energy state to another: $S_{ab}^{(v)} = S_{ab}^{(l)}$.
- When passing through two energy state transitions, the transition element satisfy:

$$S_{ab}^{(v)} = \frac{2\pi}{\mathtt{i}\hbar}\mathcal{Q}_{ba}^{(v)}\frac{A_0}{2}^2\delta(\omega_{ba}-\omega)$$

where

$$\mathcal{Q}_{ab}^{(v)} = \Big(\frac{q}{m}\Big)^2\sum_r \frac{<\phi_a|\mathbf{e}_x\cdot p|\phi_r><\phi_r|\mathbf{e}_x\cdot p|\phi_a>}{\hbar(\omega-\omega_{ra})}$$

sums over all the excited states with index r and ϕ_r are the transitions states. In the case of the length gauge we have

$$S_{ab}^{(v)} = \frac{2\pi}{\mathtt{i}\hbar}\mathcal{Q}_{ba}^{(l)}\frac{A_0}{2}^2\delta(\omega_{ba}-\omega)$$

where

$$\mathcal{Q}_{ab}^{(l)} = -\omega^2q^2\sum_r \frac{<\phi_a|\mathbf{e}_x\cdot r|\phi_r><\phi_r|\mathbf{e}_x\cdot r|\phi_a>}{\hbar(\omega-\omega_{ra})}$$

As for any ϕ_s, ϕ_t

$$<\phi_s|\mathbf{e}_x\cdot p|\phi_t>=\mathtt{i}\omega_{st}m<\phi_s|\mathbf{e}_x\cdot r|\phi_t>$$

$\mathcal{Q}_{ab}^{(l)}$ and $\mathcal{Q}_{ab}^{(v)}$ are equal as infinite series. However, in practice only a limited number of intermediate states can be evaluated. It is clear that the series $\mathcal{Q}_{ab}^{(l)}$ for ω converges more rapidly than $\mathcal{Q}_{ab}^{(v)}$ due to the fact that in general ω^2 is much smaller than $\omega_{br}\omega_{ra}$ for energy states ϕ_r such that $|E_r-E_a|\gg 1$ and $|E_r-E_b|\gg 1$. This view of non-equivalence in the gauges due to numerics brings us to the motivation of selecting each gauge.

5.5 Motivation of Gauge Selection

The velocity gauge is the most commonly used gauge to model the TDSE in practice today. The main reasoning behind this choice is that the gauge is the result of selecting the Coulomb Lagrangian. In a sense, it is the most natural choice of gauge since we do not manipulate or transform another equation to arrive at the velocity gauge.
In the length gauge representation, the particle Hamiltonian, H^l represents the the sum of the kinetic and Coulomb energies. The eigenstates ϕ_a of H^l with eigenvalue E_a are now the physical states where the energy of the particles has a well-defined value E_a. The amplitudes, $\langle\phi_b|U^{(2)}(t_f,t_0)|\phi_a\rangle$

are the real transition amplitudes from one energy level to the next where t_f and t_0 are the times at energy state E_b and E_a

The length gauge illustrates the interaction Hamiltonian as, $H^l = -x \cdot \mathbf{E}(0,t)$, which is much less complex than the interaction Hamiltonian for the velocity gauge. The length gauge interaction Hamiltonian reduces to a single algebraic term in the fields. It depends on the field $\mathbf{E}$ and not on the potentials.

We must be cautious in the use of this gauge. Although we can clearly see some advantages of its use, there are as well disadvantages. The large disadvantage of this length gauge is the term in the TDSE, $x \cdot \mathbf{E}(t)\psi$. The reason that is term brings problems is that for a large domain, x becomes very large and will be a large source of error for the numerical results.

Lastly, let us recall that the electric field $\mathbf{E}$ in the length gauge only depends on time and not space however in the velocity gauge, the electric potential $\mathbf{A}$ is dependent on time and space. When we transformed the velocity gauge into the length gauge, we assumed that the $\mathbf{A}$ was only depedent on t. In order to allow the electric field to depend on space, we would have to return to the velocity gauge where our electric potential $\mathbf{A}(x,t)$ depends on time and space. Although this new dependence seems simple, the transformation may no longer lead to the same simplicity as the length gauge previously resulted in.

6 Theory and Analysis

In this chapter, we discuss the finite difference schemes that are used to approximate the TDSEs for the length and velocity gauge. Since it is not the purpose of this paper, we only briefly describe the solving of the Maxwell equations. We then go into detail of the consistency, stability and convergence of the finite difference scheme for the velocity gauge. As well, we discuss a second approach for solving the TDSE.

6.1 Maxwell Equations

The Maxwell equations are solved by using the Yee scheme [6] which is of order two in space and time. The electric potential, $\mathbf{A}^n = \mathbf{A}(t_n)$, is computed from the Maxwell equations at each time step.

6.2 Velocity Gauge Scheme

We recall that the TDSE for the velocity gauge can be written as:

$$\mathtt{i}\partial_t\psi(x,t) = \left[-\frac{1}{2}\Delta_x + V_c(x,R_0) - \frac{\mathtt{i}}{c}\mathbf{A}(t)\cdot\nabla_x + \frac{\|\mathbf{A}(t)\|^2}{2c^2}\right]\psi(x,t) \quad (6.1)$$

where $x \in \mathbb{R}$, $t \in \mathbb{R}^+$ and $V_c(x,R_0)$ is the coulomb potential at location x, R_0 is the distance between two nuclei. The numerical scheme implemented to approximate the velocity gauge is:

$$\begin{aligned}\mathtt{i}\frac{\psi_j^{n+1}-\psi_j^n}{\Delta t} &= \frac{\psi_{j+1}^{n+1}-2\psi_j^{n+1}+\psi_{j-1}^{n+1}}{4\Delta x^2} + \frac{\psi_{j+1}^{n}-2\psi_j^{n}+\psi_{j-1}^{n}}{4\Delta x^2} \\ &\quad +\mathtt{i}\mathbf{A}^n\left(\frac{\psi_{j+1}^{n+1}-\psi_{j-1}^{n+1}}{4\Delta x} + \frac{\psi_{j+1}^{n}-\psi_{j-1}^{n}}{4\Delta x}\right) \end{aligned} \quad (6.2)$$

where Δx represents the (fixed) space step size, Δt is the time step size, $\mathbf{A}^n$ is the electric potential at a time t_n and ψ_j^n is the solution (dipole moment) at time j and location n. In the following subsections we will see that we use this scheme since it has some strong properties.

6.2.1 Stability

Stability of a finite difference scheme indicates if the error produced is bounded. Three possibilities are: always bounded, bounded under some condition on space, Δx and time Δt, or unbounded. In scientific terms they

are unconditionally stable, stable with a Courant, Friedrichs, Lewy (CFL) condition, or unstable respectively. In order to study the stability of our finite difference scheme we carry out the classical approach and take a close look at the amplification factor, $g(\theta)$, where $\theta \in (-\frac{\pi}{\Delta x}, \frac{\pi}{\Delta x})$. Amplification factor is so called because its magnitude is the amount that the amplitude of each frequency in the solution is amplified in advancing the solution one time step [9]. It indicates under what conditions the scheme will remain stable. The amplification factor, $g(\theta)$, needs to satisfy $|g(\theta)| \leq 1$ in order for the scheme to be stable $\forall \theta \in (-\frac{\pi}{\Delta x}, \frac{\pi}{\Delta x})$. Rigorous stability analysis involves applying the Fourier transform of the scheme, however it can be proved [9] that replacing ψ_j^n with $g(\theta)^n e^{ij\theta}$ within the scheme is equivalent. After this replacement, we solve for $g(\theta)$ and verify under what conditions the scheme is stable.

$$\begin{aligned}\frac{\mathtt{i}}{\Delta t}\left(g^{n+1}(\theta)e^{\mathtt{i}j\theta} - g^n(\theta)e^{\mathtt{i}j\theta}\right) &= \frac{1}{4\Delta x^2}\left(g^{n+1}(\theta)e^{\mathtt{i}(j+1)\theta} - 2g^{n+1}(\theta)e^{\mathtt{i}j\theta} + g^{n+1}(\theta)e^{\mathtt{i}(j-1)\theta}\right)\\ &+\frac{1}{4\Delta x^2}\left(g^{n}(\theta)e^{\mathtt{i}(j+1)\theta} - 2g^{n}(\theta)e^{\mathtt{i}j\theta} + g^{n}(\theta)e^{\mathtt{i}(j-1)\theta}\right)\\ &+\frac{\mathtt{i}\mathbf{A}^n}{4\Delta x}\left(g^{n+1}(\theta)e^{\mathtt{i}(j+1)\theta} - g^{n+1}(\theta)e^{\mathtt{i}(j-1)\theta}\right)\\ &+\frac{\mathtt{i}\mathbf{A}^n}{4\Delta x}\left(g^{n}(\theta)e^{\mathtt{i}(j+1)\theta} - g^{n}(\theta)e^{\mathtt{i}(j-1)\theta}\right).\end{aligned}$$

We then divide both sides of the equation by $g(\theta)^n e^{\mathtt{i}j\theta}$

$$\begin{aligned}\frac{\mathtt{i}}{\Delta t}\left(g(\theta) - 1\right) &= \frac{1}{4\Delta x^2}\left(g(\theta)e^{\mathtt{i}\theta} - 2g(\theta) + g(\theta)e^{-\mathtt{i}\theta}\right) + \frac{1}{4\Delta x^2}\left(e^{\mathtt{i}\theta} - 2 + e^{-\mathtt{i}\theta}\right)\\ &+\frac{\mathtt{i}\mathbf{A}^n}{4\Delta x}\left(g(\theta)e^{\mathtt{i}\theta} - g(\theta)e^{-\mathtt{i}\theta}\right) + \frac{\mathtt{i}\mathbf{A}^n}{4\Delta x}\left(e^{\mathtt{i}\theta} - e^{-\mathtt{i}\theta}\right).\end{aligned}$$

We recall Euler's identity : $e^{\mathtt{i}\theta} = \cos\theta + \mathtt{i}\sin\theta$

$$\begin{aligned}\frac{\mathtt{i}}{\Delta t}\left(g(\theta) - 1\right) &= \frac{g(\theta)}{4\Delta x^2}\left(2\cos\theta - 2\right) + \frac{1}{4\Delta x^2}\left(2\cos\theta - 2\right)\\ &+\frac{\mathtt{i}\mathbf{A}^n g(\theta)}{4\Delta x}\left(2\mathtt{i}\sin\theta\right) + \frac{\mathtt{i}\mathbf{A}^n}{4\Delta x}\left(2\mathtt{i}\sin\theta\right).\end{aligned}$$

We then isolate for amplification factor $g(\theta)$:

$$g(\theta)\left[\frac{\mathtt{i}}{\Delta t} - \frac{\cos\theta - 1}{2\Delta x^2} + \frac{\mathbf{A}^n\sin\theta}{2\Delta x}\right] = \frac{\mathtt{i}}{\Delta t} + \frac{\cos\theta - 1}{2\Delta x^2} - \frac{\mathbf{A}^n\sin\theta}{2\Delta x}$$

$$g(\theta) = \frac{\dfrac{\mathtt{i}}{\Delta t} - \dfrac{\cos\theta - 1}{2\Delta x^2} - \dfrac{\mathbf{A}^n\sin\theta}{2\Delta x}}{\dfrac{\mathtt{i}}{\Delta t} + \dfrac{\cos\theta - 1}{2\Delta x^2} + \dfrac{\mathbf{A}^n\sin\theta}{2\Delta x}}$$

Now we wish to compute $|g(\theta)|^2$.

$$
\begin{aligned}
|g(\theta)|^2 &= \left| \frac{\frac{\mathtt{i}}{\Delta t} - \frac{\cos\theta - 1}{2\Delta x^2} - \frac{\mathbf{A}^n \sin\theta}{2\Delta x}}{\frac{\mathtt{i}}{\Delta t} + \frac{\cos\theta - 1}{2\Delta x^2} + \frac{\mathbf{A}^n \sin\theta}{2\Delta x}} \right|^2 \\
&= \frac{\left| \frac{\mathtt{i}}{\Delta t} - \frac{\cos\theta - 1}{2\Delta x^2} - \frac{\mathbf{A}^n \sin\theta}{2\Delta x} \right|^2}{\left| \frac{\mathtt{i}}{\Delta t} + \frac{\cos\theta - 1}{2\Delta x^2} + \frac{\mathbf{A}^n \sin\theta}{2\Delta x} \right|^2} \\
&= \frac{\left(\frac{\mathtt{i}}{\Delta t} \right)^2 + (-1)^2 \left(\frac{\cos\theta - 1}{2\Delta x^2} + \frac{\mathbf{A}^n \sin\theta}{2\Delta x} \right)^2}{\left(\frac{\mathtt{i}}{\Delta t} \right)^2 + \left(\frac{\cos\theta - 1}{2\Delta x^2} + \frac{\mathbf{A}^n \sin\theta}{2\Delta x} \right)^2} \\
&= 1
\end{aligned}
$$

Hence the amplification factor $|g(\theta)|^2 = 1$, for Δx, Δt and $\forall\theta \in \left[-\frac{\pi}{\Delta x}, \frac{\pi}{\Delta x}\right]$, therefore the scheme is unconditionally stable.

6.2.2 Consistency

We consider the consistency of the finite difference scheme (6.2). In order to evaluate the consistency, we take a smooth solution ϕ and take the Taylor

expansions.

$$\phi_j^{n+1} = \phi_j^n + \Delta t \phi_{t,j}^n + \frac{\Delta t^2}{2}\phi_{tt,j}^n + \mathcal{O}(\Delta t^3) \tag{6.3}$$

$$\phi_{j+1}^n = \phi_j^n + \Delta x \phi_{x,j}^n + \frac{\Delta x^2}{2}\phi_{xx,j}^n + \frac{\Delta x^3}{6}\phi_{xxx,j}^n + \mathcal{O}(\Delta x^4) \tag{6.4}$$

$$\phi_{j-1}^n = \phi_j^n - \Delta x \phi_{x,j}^n + \frac{\Delta x^2}{2}\phi_{xx,j}^n - \frac{\Delta x^3}{6}\phi_{xxx,j}^n + \mathcal{O}(\Delta x^4) \tag{6.5}$$

$$\begin{aligned}\phi_{j+1}^{n+1} = \phi_j^n + \Delta x \phi_{x,j}^n + \Delta t \phi_{t,j}^n + \frac{\Delta x^2}{2}\phi_{xx,j}^n + 2\Delta x \Delta t \phi_{xt,j}^n + \frac{\Delta t^2}{2}\phi_{tt,j}^n + \frac{\Delta t \Delta x^2}{2}\phi_{xxt,j}^n \\ + \frac{\Delta x \Delta t^2}{2}\phi_{xtt,j}^n + \mathcal{O}(\Delta x^3) + \mathcal{O}(\Delta t^3)\end{aligned} \tag{6.6}$$

$$\begin{aligned}\phi_{j-1}^{n+1} = \phi_j^n - \Delta x \phi_{x,j}^n + \Delta t \phi_{t,j}^n + \frac{\Delta x^2}{2}\phi_{xx,j}^n - 2\Delta x \Delta t \phi_{xt,j}^n + \frac{\Delta t^2}{2}\phi_{tt,j}^n + \frac{\Delta t \Delta x^2}{2}\phi_{xxt,j}^n \\ - \frac{\Delta x \Delta t^2}{2}\phi_{xtt,j}^n + \mathcal{O}(\Delta x^3) + \mathcal{O}(\Delta t^3)\end{aligned} \tag{6.7}$$

where j and t_n represent the time and space location respectively. $\mathcal{O}$ is the big O notation where $\mathcal{O}(g(x))$ for some function $g(x)$, $\exists x_0, c \in \mathbb{R}$ such that $\phi \leq cg(x)$, $\forall x > x_0$.
Now we replace the terms in the finite difference scheme with their appropriate Taylor expansions as follows:

$$\begin{aligned}\frac{\mathtt{i}}{\Delta t}\left(\Delta t \phi_{t,j}^n + \frac{\Delta t^2}{2}\phi_{tt,j}^n + \mathcal{O}(\Delta t^3)\right) = \frac{1}{4\Delta x^2}\left(\Delta x^2 \phi_{xx,j}^n + \frac{1}{2}\Delta x^2 \Delta t \phi_{xxt,j}^n + \mathcal{O}(\Delta x^4)\right) \\ + \frac{1}{4\Delta x^2}\left(\Delta x^2 \phi_{xx,j}^n + \mathcal{O}(\Delta x^4)\right) \\ + \frac{\mathtt{i}\mathbf{A}^n}{4\Delta x}\left(2h\phi_{x,j}^n \Delta x \Delta t \phi_{xt,j}^n + \mathcal{O}(\Delta x \Delta t^2) + \mathcal{O}(\Delta x^3)\right) \\ + \frac{\mathtt{i}\mathbf{A}^n}{4\Delta x}\left(2\Delta x \phi_{x,j}^n + \mathcal{O}(\Delta x^3)\right)\end{aligned} \tag{6.8}$$

$$\begin{aligned}
\mathtt{i}\phi^n_{t,j} + \mathtt{i}\frac{\Delta t}{2}\phi^n_{tt,j} + \mathcal{O}(\Delta t^2) &= \frac{1}{4}\phi^n_{xx,j} + \frac{1}{4}\Delta t\phi^n_{xxt,j} + \mathcal{O}(\Delta x^2) + \frac{1}{4}\phi^n_{xx,j} + \mathcal{O}(\Delta x^2) \\
&\quad + \mathtt{i}\mathbf{A}^n\left(\frac{1}{2}\phi^n_{x,j} + \frac{\Delta t}{2}\phi^n_{xt,j}\right) + \mathcal{O}(\Delta t^2) + \mathcal{O}(\Delta x^2) \\
&\quad + \mathtt{i}\mathbf{A}^n\left(\frac{1}{2}\phi^n_{x,j} + \mathcal{O}(\Delta x^2)\right) \\
&= \frac{1}{2}\phi^n_{xx,j} + \mathcal{O}(\Delta x^2) + \mathtt{i}\mathbf{A}^n\phi^n_{x,j} + \mathcal{O}(\Delta t^2) + \frac{\Delta t}{4}\phi^n_{xxt,j} \\
&\quad + \mathtt{i}\mathbf{A}^n\frac{\Delta t}{2}\phi^n_{xt,j} \qquad (6.9)
\end{aligned}$$

The differential equation we are trying to approximate is:

$$\mathtt{i}\phi_t = \mathtt{i}\mathbf{A}^n\phi_x + \frac{1}{2}\phi_{xx} \qquad (6.10)$$

and if we take the derivative with respect to t and multiply by $\Delta t/2$ and sum this with equation (6.10) we will obtain equation (6.9) which reduces to:

$$\mathtt{i}\phi^n_{t,j} = \mathtt{i}\mathbf{A}^n\phi^n_{x,j} + \frac{1}{2}\phi^n_{xx,j} + \mathcal{O}(\Delta x^2) + \mathcal{O}(\Delta t^2). \qquad (6.11)$$

Hence, the scheme is of order (2,2) with respect to time and space.

6.2.3 Convergence

In reference to the finite difference scheme used for the velocity gauge, we see that it is stable with an amplification factor $|g(\theta)|^2 = 1$, and accurate at order (2,2) in time and space. In conclusion, the scheme is convergent.

6.3 Length Gauge Scheme

We recall that the TDSE in the length gauge is written:

$$\mathtt{i}\partial_t\psi(x,t) = \left[-\frac{1}{2}\Delta_x + V_c(x,R_0) + x\mathbf{E}(t)\right]\psi(x,t).$$

Within the code, which is discussed thoroughly in a later chapter, the final term $x\mathbf{E}(t)\psi(x,t)$ is computed seperately from the rest of the equation. We split the TDSE into two parts and use the finite difference scheme described to approximate part of the equation, and solve the other part involving the final term $x\mathbf{E}(t)\psi(x,t)$. The finite difference scheme used to approximate the length gauge is:

$$\mathtt{i}\frac{\psi^{n+1}_j - \psi^n_j}{\Delta t} = \frac{\psi^{n+1}_{j+1} - 2\psi^{n+1}_j + \psi^{n+1}_{j-1}}{4\Delta x^2} + \frac{\psi^n_{j+1} - 2\psi^n_j + \psi^n_{j-1}}{4\Delta x^2} \qquad (6.12)$$

where Δx represents the space step size, Δt is the time step size, $\mathbf{E}(t)$ is the electric field at time t and ψ_j^n is the solution at time j and time t_n
The numerical analysis for the length gauge finite difference scheme has the same results as the previous velocity gauge scheme. In regards to the stability analysis of this scheme, it can be proved that the amplification factor is equal to 1. As well, the scheme is consistent of order 2 in time and space. We can conclude that the scheme is convergent since it is both stable and consistent.

6.4 Velocity Gauge Scheme Alternative Approach

The previous analysis illustrates the strength of the finite difference scheme that is being applied. However, this is not the only choice that is available in order to solve the TDSE. The length gauge was solved previously by a splitting method. We split our equation in two parts, where one equation depends on the solution of the other. We could approach solving the velocity gauge TDSE in a similar manner.

6.4.1 Strang Splitting Method

The splitting method involves partitioning the equation into one or more parts. Let A and B be algebraic or differential operators and ψ is a smooth function, and consider the equation:

$$\begin{cases} \partial_t \psi(x,t) = (A+B)\psi(x,t), \quad \psi(t_n,\cdot) = \psi^n \quad t \in [t_n, t_n + \Delta t) \\ \psi(x,0) = \psi_0 \end{cases}$$

Now, for illustration purposes, let us consider A and B as matrices. The equation is merely an ordinary differential equation, and the solution is in the form $\exp(A+B)$. Let us recall that the exponential of a matrix is defined as an infinite sum:

$$\begin{aligned} \exp(A) &= \sum_{k=0}^{\infty} \frac{1}{k!} A^k \\ &= \mathbb{I} + A + \frac{1}{2}A^2 + \frac{1}{6}A^3 + \dots \end{aligned}$$

Strang splitting begins by partitioning the original equation as follows:

$$\begin{aligned} &\partial_t \psi = A\psi, \quad \psi(t_n,\cdot) = \psi^n, \qquad t \in [t_n, t_{n^*}) \\ &\partial_t \psi = B\psi, \quad \psi(t_{n^*},\cdot) = \psi^{n^*}, \qquad t \in [t_{n^*}, t_{n^{**}}) \\ &\partial_t \psi = A\psi, \quad \psi(t_n^{**},\cdot) = \psi^{n^{**}}, \quad t \in [t_{n^{**}}, t_n + \Delta t) \end{aligned} \tag{6.13}$$

This leads to:

$$\exp\left(\frac{\Delta t}{2}A\right)\exp(\Delta t B)\exp\left(\frac{\Delta t}{2}A\right)$$

If we expand this solution we obtain:

$$\begin{aligned}
&\left(\mathbb{I}+\frac{\Delta t}{2}A+\frac{\Delta t^2}{8}A^2+\mathcal{O}(\Delta t^3)\right)\cdot\left(\mathbb{I}+\Delta t B+\frac{\Delta t^2}{2}B^2+\mathcal{O}(\Delta t^3)\right)\cdot\left(\mathbb{I}+\frac{\Delta t}{2}A+\frac{\Delta t^2}{8}A^2+\mathcal{O}(\Delta t^3)\right)\\
&=\left(\mathbb{I}+\frac{\Delta t}{2}A+\Delta t B+\frac{\Delta t^2}{2}AB+\mathcal{O}(\Delta t^3)\right)\cdot\left(\mathbb{I}+\frac{\Delta t}{2}A+\frac{\Delta t^2}{8}A^2+\mathcal{O}(\Delta t^3)\right)\\
&=\mathbb{I}+\Delta t A+\Delta t B+\frac{\Delta t^2}{2}BA+\frac{\Delta t^2}{2}AB+\frac{\Delta t^2}{2}AB+\mathcal{O}(\Delta t^3)
\end{aligned}$$

Returning to the original equation, the solution is in the form:

$$\exp(A+B)=\mathbb{I}+\Delta t B+\Delta t A+\frac{\Delta t^2}{2}B+\frac{\Delta t^2}{2}A+\frac{\Delta t^2}{2}AB+\frac{\Delta t^2}{2}BA+\mathcal{O}(\Delta t^3)$$

Hence, this method is used to avoid the issue of when A and B do not commute i.e. $AB = BA$. At each time iteration, an error of $\mathcal{O}(\Delta t^3)$ is produced and so it has a global error of $\mathcal{O}(\Delta t^2)$ by the time-splitting [4].

6.4.2 Splitting Method for Velocity Gauge

Using the velocity gauge, our equation can be rewritten as follows:

$$\partial_t\psi(x,t)=\left[\frac{\mathtt{i}}{2}\Delta_x-\mathtt{i}V_c(x,R_0)-\frac{1}{c}\mathbf{A}(t)\cdot\nabla_x-\mathtt{i}\frac{\|\mathbf{A}(t)\|^2}{2c^2}.\right]\psi(x,t)$$

We split into:

$$\partial_t\psi(x,t)=B\psi(x,t)+D\psi(x,t),$$

where

$$\begin{cases}B &= \frac{\mathtt{i}}{2}\Delta_r-\mathtt{i}V_c(x,R_0),\\ D &= -\frac{1}{c}\mathbf{A}(t)\cdot\nabla_x-\mathtt{i}\frac{\|\mathbf{A}(t)\|^2}{2c^2}.\end{cases}$$

We then carry out the Strang splitting described in equation (6.13) in order to solve the TDSE.

6.4.3 Method of Characteristics

The method of characteristics is a classical method for in particular, solving linear advection (or transport) equations. Advection equations are both linear and hyberbolic. When we solve the TDSE used for the velocity gauge, we apply the Strang splitting method. The first part of the splitting is solved by approximating the equation with a finite difference scheme. The second part of the splitting method is the following:

$$\mathtt{i}\partial_t\psi(x,t) = -\mathtt{i}\mathbf{A}\partial_x\psi(x,t).$$

Remark 1. *Although we treat* $\mathbf{A}$ *independent of the variable* t*,* $\mathbf{A}$ *is indeed dependent on the variable* t*. By taking the approximation of* t *as* t_n *and using the Taylor expansion, from the term involving the* ∂_x*, with* $\delta \ll 1$ *we obtain:*

$$\mathbf{A}(t) = \mathbf{A}(t_n) + \mathcal{O}\left(\|\mathbf{A}'(t_n)\|\delta t\right).$$

Numerically, we approximate the advection equation using the upwind scheme. Since $\mathbf{A}$ is a variable, we check whether it is positive or negative in order to determine whether we can use the forward or backward approximation when iterating through t_n as $n \mapsto \infty$, Δx is the space step, and Δt is the time step.

$$\mathtt{sgn}(A) = \begin{cases} = 1 \;\; if \;\; A > 0 \\ = -1 \;\; if \;\; A < 0 \\ = 0 \;\; if \;\; A = 0 \end{cases}$$

$$\frac{\psi_j^{n+1} - \psi_j^n}{\Delta t} = \mathbf{A}(t_n)\frac{1 - \mathtt{sgn}(\mathbf{A}(t_n))}{2}\frac{\psi_{j+1}^n - \psi_j^n}{\Delta x} + \mathbf{A}(t_n)\frac{1 + \mathtt{sgn}(\mathbf{A}(t_n))}{2}\frac{\psi_j^n - \psi_{j-1}^n}{\Delta x}$$

6.4.4 Consequences

The broad concept of applying the splitting method and method of characteristics to solve our velocity gauge TDSE appears to result in a very simple and elegant approach. Unfortunately, when we begin to apply this method more thoroughly we unravel many computational difficulties.
In order for the upwind scheme to remain stable, the CFL condition

$$\frac{\|\mathbf{A}(t_n)\|\Delta t_n}{\Delta x} = 1$$

needs to be upheld with a nonconstant time step. In the case of the length gauge, the electric field, $\mathbf{E}$, is constant and so once we select our time and

space size, the time step is a constant. However, for the velocity gauge, the electric potential is dependent on time and hence varies for each Maxwell equation that is solved. Moreover, the time step in the velocity gauge is changing depending on the iteration number and the current space coordinate where the equation is being solved. i.e. Δt. The time step is changing at ever time iteration.
The previous TDSE that was solved within the code was the length gauge. We attempted to replace the length gauge solver by the velocity gauge TDSE solver. The code for solving the length gauge involves the Maxwell and Schrödinger time steps ratio, $N_i = \dfrac{\Delta t^{Maxw}}{\Delta t_i^{Schro}}$, in order to determine the number of iterations needed to solve the TDSE in the given domain. A visual description of the code for the length gauge appears as:

```
...
for (int i=0; i<numOfMaxwell; i++) /* Maxwell iterations*/
{
...
 for(int j =0; j<ratioOfMaxSchro; j++) /* Schrodinger iterations*/
 {
 update(...,ratioOfMaxSchro ,...);
 }
...
}
...
```

where we see that the ratio of Maxwell to Schrödinger equations is used as an ending condition in the nested for loop. We use this value again when updating the current electric field at each time iteration.
Whereas in the length gauge this ratio was constant, in the velocity gauge, it is no longer the same case. This complication is a programming problem since the manner in which the length gauge code is solved is not flexible when it comes to changing N_i from a constant to a variable. Although this proposed method is still possible, it involves ones strong attention and careful attempt at the required changes.

7 Programming Aspect

7.1 Length Gauge

The way we approach solving the length gauge is the splitting method. We first use the finite difference scheme

$$\mathtt{i}\frac{\psi_j^{n+1}-\psi_j^n}{\Delta t}=\frac{\psi_{j+1}^{n+1}-2\psi_j^{n+1}+\psi_{j-1}^{n+1}}{4\Delta x^2}+\frac{\psi_{j+1}^{n}-2\psi_j^{n}+\psi_{j-1}^{n}}{4\Delta x^2} \tag{7.1}$$

in order to solve the part of the TDSE which is equivalent to:

$$\mathtt{i}\partial_t\psi(x,t)=\left[-\frac{1}{2}\Delta_x+V_c(x,R_0)\right]\psi(x,t)$$

where $V_c(x,R_0)$ is the electron-nucleus potential. Within the same solver for the TDSE, we compute the second part of the splitting which is equivalent to solving

$$\mathtt{i}\partial_t\psi(x,t)=x\mathbf{E}(t)\psi(x,t)$$

7.2 Velocity Gauge

In order to solve the TDSE for the velocity gauge:

$$\mathtt{i}\partial_t\psi(x,t)=\left[-\frac{1}{2}\Delta_x+V_c(x,R_0)-\frac{\mathtt{i}}{c}\mathbf{A}(t)\cdot\nabla_x+\frac{\|\mathbf{A}(t)\|^2}{2c^2}\right]\psi(x,t) \tag{7.2}$$

the linear system of equations we need to solve is in the form:

$$A^n\psi^{n+1}=B^n\psi^n$$

$A^n\in M_{2N\times 2N}(\mathbb{C})$, $B^n\in M_{2N\times 2N}(\mathbb{C})$ and $\psi^n\in\mathbb{C}^{2N}$, where N is the number of Maxwell equations we need to solve for the system described in section (2.2). Now, we separate the system into its corresponding real (R) and imaginary parts (I).

$$\begin{cases} A^n &= A_R^n+\mathtt{i}A_I^n \\ B^n &= B_R^n+\mathtt{i}B_I^n \\ \psi^n &= \psi_R^n+\mathtt{i}\psi_I^n \end{cases}$$

We then substitute these equations into the original system and in a more compact version obtain the following:

$$\left[\begin{array}{c|c} A_R^n & -A_I^n \\ \hline A_I^n & A_R^n \end{array}\right]\left[\begin{array}{c} \psi_R^{n+1} \\ \psi_I^{n+1} \end{array}\right]=\left[\begin{array}{c|c} B_R^n & -B_I^n \\ \hline B_I^n & B_R^n \end{array}\right]\left[\begin{array}{c} \psi_R^{n} \\ \psi_I^{n} \end{array}\right]$$

In reference to the velocity gauge scheme discussed in section (6.1), A and B are diagonal matrices where A corresponds to the $n+1$ terms and B corresponds to the nth terms defined as follows:

$$A_R^n = \begin{bmatrix} 1 & -\frac{A^n\Delta t}{4\Delta x} & & & \\ \frac{A^n\Delta t}{4\Delta x} & 1 & -\frac{A^n\Delta t}{4\Delta x} & & 0 \\ & \ddots & \ddots & \ddots & \\ 0 & & \frac{A^n\Delta t}{4\Delta x} & 1 & -\frac{A^n\Delta t}{4\Delta x} \\ & & & \frac{A^n\Delta t}{4\Delta x} & 1 \end{bmatrix},$$

$$B_R^n = \begin{bmatrix} 1 & \frac{A^n\Delta t}{4\Delta x} & & & \\ -\frac{A^n\Delta t}{4\Delta x} & 1 & \frac{A^n\Delta t}{4\Delta x} & & 0 \\ & \ddots & \ddots & \ddots & \\ 0 & & -\frac{A^n\Delta t}{4\Delta x} & 1 & \frac{A^n\Delta t}{4\Delta x} \\ & & & -\frac{A^n\Delta t}{4\Delta x} & 1 \end{bmatrix},$$

$$A_I^n = \begin{bmatrix} \frac{\Delta t}{2\Delta x^2} & -\frac{\Delta t}{4\Delta x^2} & & & \\ -\frac{\Delta t}{4\Delta x^2} & \frac{\Delta t}{2\Delta x^2} & -\frac{\Delta t}{4\Delta x^2} & & 0 \\ & \ddots & \ddots & \ddots & \\ 0 & & -\frac{\Delta t}{4\Delta x^2} & \frac{\Delta t}{2\Delta x^2} & -\frac{\Delta t}{4\Delta x^2} \\ & & & -\frac{\Delta t}{4\Delta x^2} & \frac{\Delta t}{2\Delta x^2} \end{bmatrix},$$

$$B_I^n = \begin{bmatrix} -\frac{\Delta t}{2\Delta x^2} & \frac{\Delta t}{4\Delta x^2} & & & \\ \frac{\Delta t}{4\Delta x^2} & -\frac{\Delta t}{2\Delta x^2} & \frac{\Delta t}{4\Delta x^2} & & 0 \\ & \ddots & \ddots & \ddots & \\ 0 & & \frac{\Delta t}{4\Delta x^2} & -\frac{\Delta t}{2\Delta x^2} & \frac{\Delta t}{4\Delta x^2} \\ & & & \frac{\Delta t}{4\Delta x^2} & -\frac{\Delta t}{2\Delta x^2} \end{bmatrix}.$$

Within our block system of equations, we solve for ψ^{n+1} and we are given Δt which is the time step, Δx which is the step size, and $\mathbf{A}^n$ is the electric potential at time t_n.
In this paper, we are modifying the previous length gauge solver into the velocity gauge solver. Let us recall that we solve the length gauge in two parts and since the second part involving $x\mathbf{E}(t)\psi(x,t)$ is no longer in the velocity gauge, we merely delete this portion of the solver, and only need to add to the two new terms into our finite difference scheme. This is a consequence of the fact that both length and velocity gauges have the common two terms

$$\left[-\frac{1}{2}\Delta_x + V_c(x, R_0)\right]\psi(x,t).$$

Then the two new terms in the velocity gauge then correspond to adding values along the upper and lower diagonals of the real matrices A and B. Hence, from a programming perspective, the changes are not difficult due to the set up of the length gauge code.

7.3 Parallel Computing

Let us briefly recall from section 2, the discussion of the Maxwell-Schrödinger model. Firstly, computation of many TDSEs lead to the computation of the polarization which in turn allows us to solve the Maxwell equations giving a solution in the form of the electric and magnetic field, $(\mathbf{E}, \mathbf{B})$. We repeat the steps using the updated electric field in the TDSEs. We can clearly see that as the number of Schrödinger equations increases, the number of computations needed to solve the system grows very large. This brings rise to the motivation to use parallel programming, in order to divide the

problem among many processors and decrease the overall time needed for numerical computation. The computational scheme can be broken down into the following steps [5]:

1. From time t^n to t^{n^*} we solve l TDSE's on m processors. Each TDSE is solved sequentially (l/m TDSE's per processor). We then calculate the polarization, $\mathbf{P}$.

2. Local polarization are sent to the nodes in charge of the Maxwell equation computation, more precisely, the nodes in charge of the gas regions.

3. From t^{n^*} to $t^{n^{**}}$ the current density $\overrightarrow{\mathbf{j}}$ (3.1) is updated by solving a differential equation.

4. From $t^{n^{**}}$ to t^{n+1} we solve by domain decomposition the Maxwell equations, on $N_p - m$ processors where N_p is the total number of processors.

We take $N_p = 8$ and $m = 5$ for the following diagram:

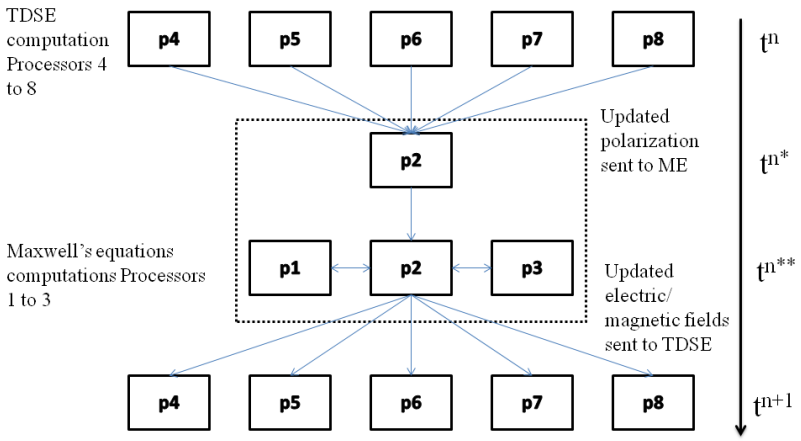

Figure 5: Parallelism that is involved in solving the Maxwell-Schrödinger coupling.

8 Numerical Simulation

8.1 Comparison

Subsequently from the analysis of the finite difference scheme that is used to approximate the velocity gauge, the scheme is indeed convergent. With this in mind, along with gauge theory and local gauge invariance, we expect the solution under the velocity gauge framework to be consistent with the results from the length gauge framework. Our linear system that is solved gives us the harmonics as its physical significance. For the purposes of this paper, the initial data may or may not have physical significance however, the objective is to illustrate that the velocity and length gauge produce consistent results (whether or not they have physical signficance is not of importance).

8.2 Incoming and Outgoing Electric Field

The laser pulse or electric field that first interacts with the gas of molecules is explicity computed. The incoming electric field is a choice created by the user. The more molecules in the gas we consider will change the outgoing electric field. The molecules effect the laser that is interacting with the gas, and hence, with more molecules comes a change in the outgoing electric field. The incoming pulse we use is:

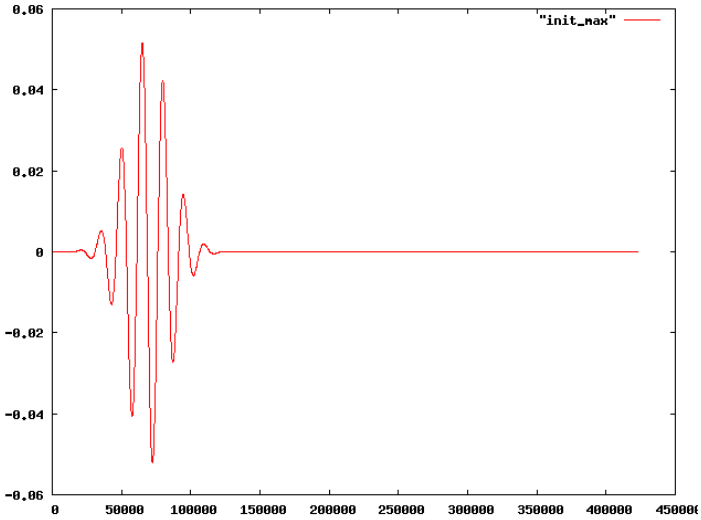

Figure 6: This figure illustrates the incoming pulse we use for both 8 molecules and 96 molecules

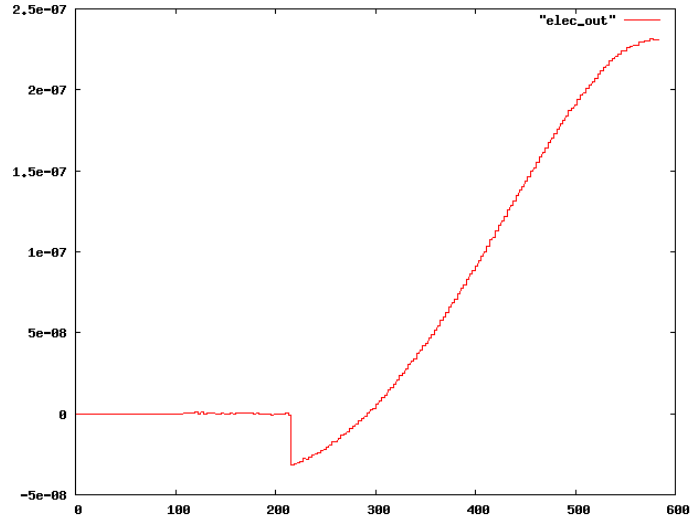

Figure 7: This figure illustrates the outgoing electric field for 8 molecules

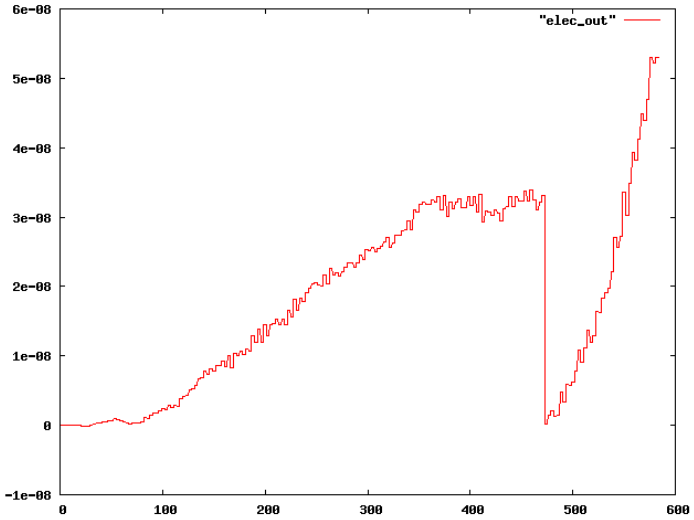

Figure 8: This figure illustrates the outgoing electric field for 96 molecules

8.3 Harmonics

In addition, the model also computes the harmonics of the system. Both the harmonics for the electric field and the dipole moment are computed. The harmonics correspond to the odd multiples of ω_0. Most nonlinear optics models only consider the first three orders, whereas we compute N-orders. Due to regularization we obtain values between the odd multiples, however the true values correspond to the peaks which are located at these odd multiples of ω_0. We compare the length and velocity gauge harmonics of the dipole moment and electric field for few molecules and for a large amount. Once more, let us recall that the initial data does not necessarily have physical significance and thus the harmonics spectrum is not consistent with the usual description and meaning. The goal of this section is to demonstrate that the theory coincides with the numerical data and we should obtain consistent results when comparing the length gauge to the velocity gauge.

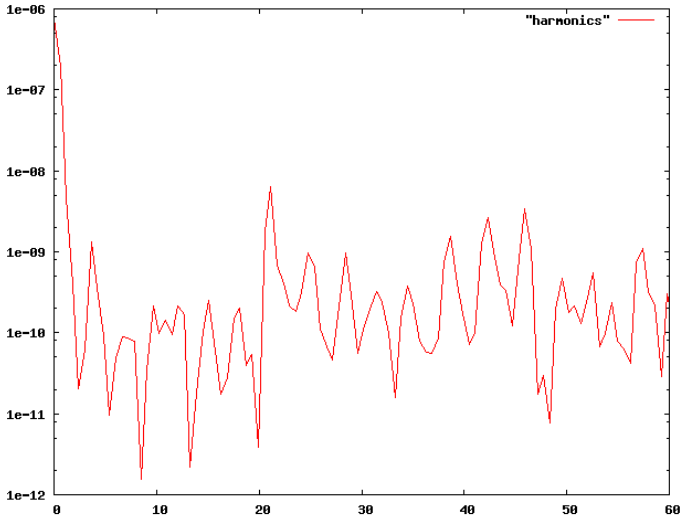

Figure 9: This figure illustrates the harmonics of the dipole moment for 8 molecules in the length gauge

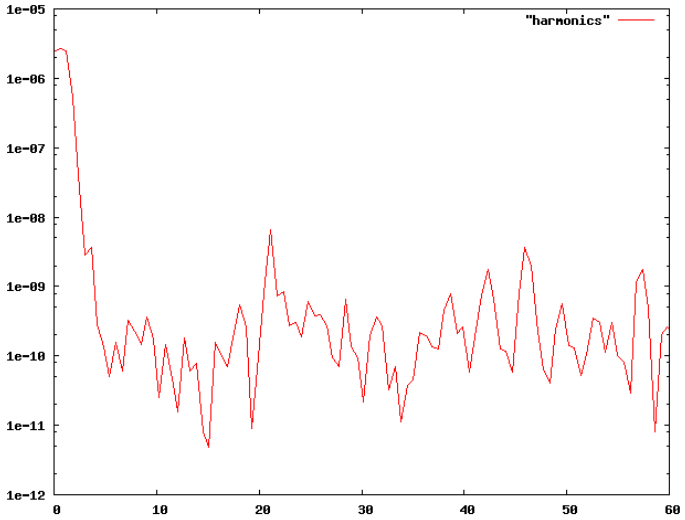

Figure 10: This figure illustrates the harmonics of the dipole moment for 8 molecules in the velocity gauge

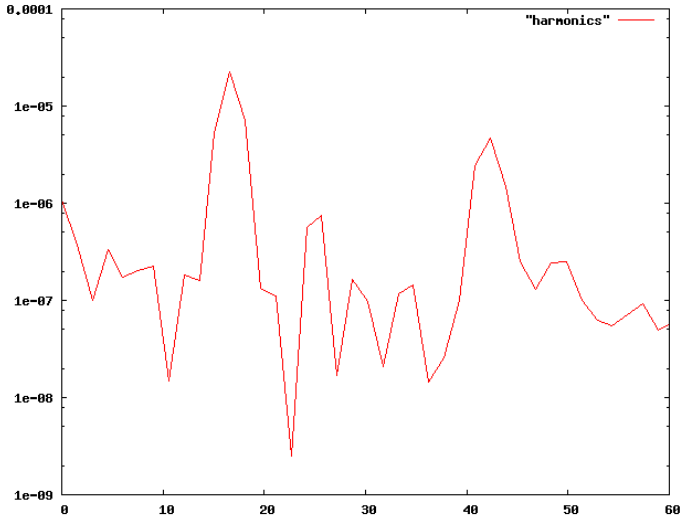

Figure 11: This figure illustrates the harmonics of the dipole moment for 96 molecules in the length gauge

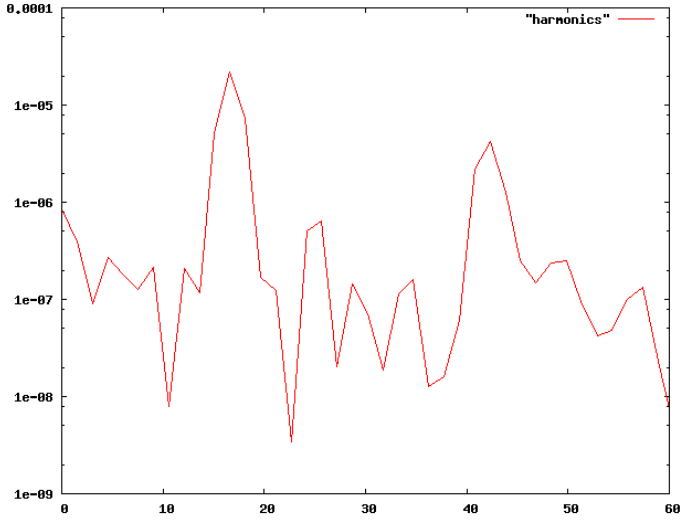

Figure 12: This figure illustrates the harmonics of the dipole moment for 96 molecules in the velocity gauge

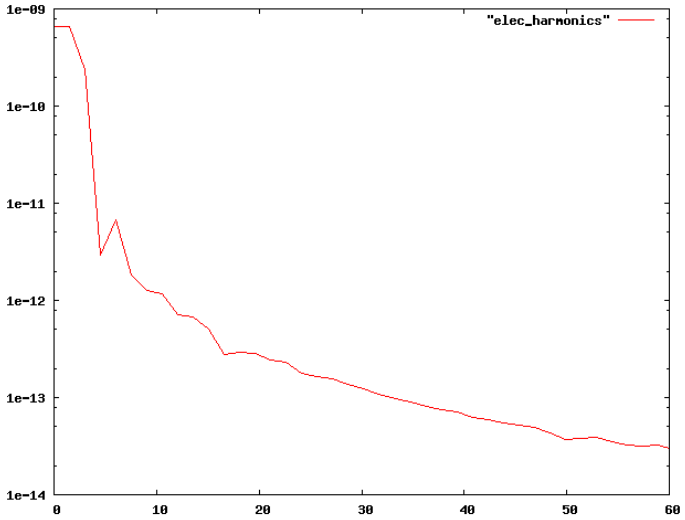

Figure 13: This figure illustrates the harmonics of the electric field for 8 molecules in the length gauge

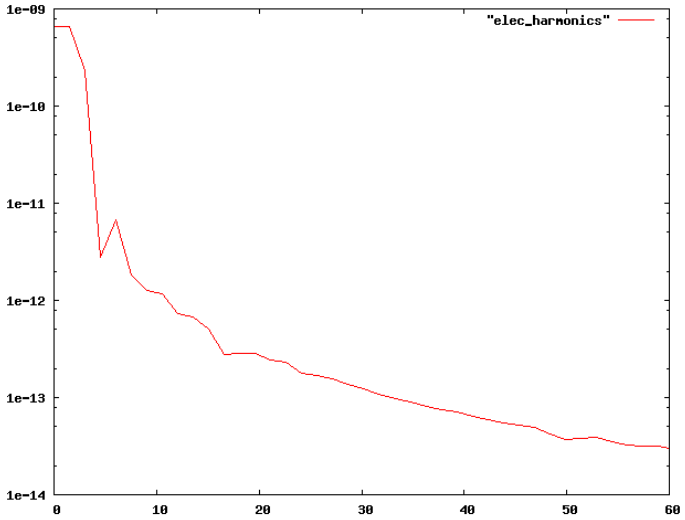

Figure 14: This figure illustrates the harmonics of the electric field for 8 molecules in the velocity gauge

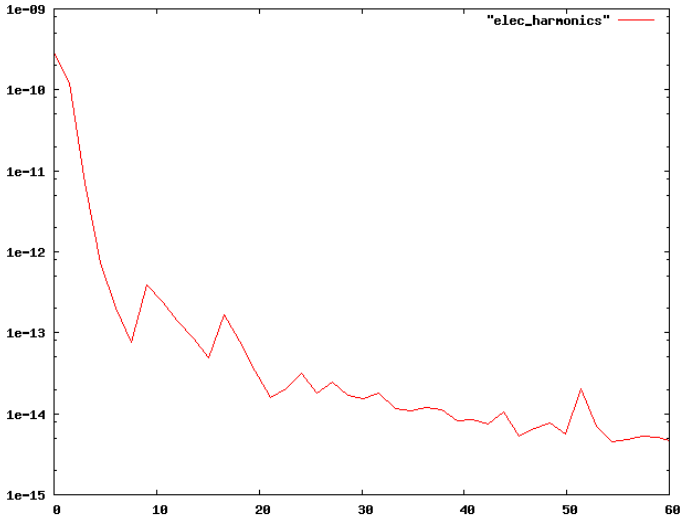

Figure 15: This figure illustrates the harmonics of the electric field for 96 molecules in the length gauge

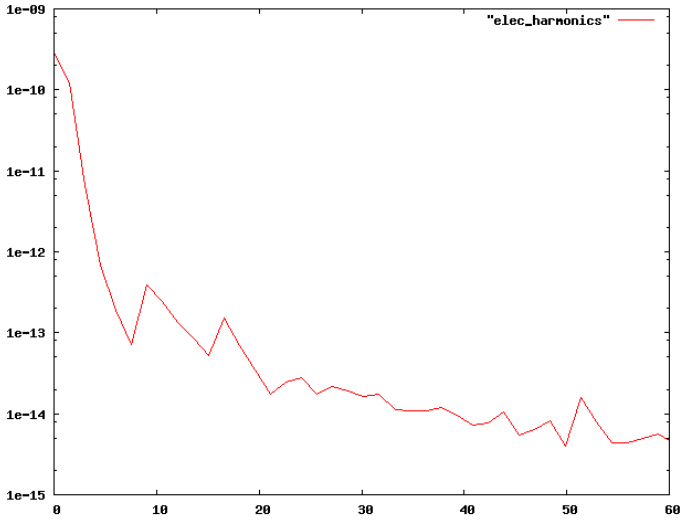

Figure 16: This figure illustrates the harmonics of the electric field for 96 molecules in the velocity gauge

8.4 Probability of the Electrons Position

Within this framework, we work with $H_2^{\pm}$ molecule gas fixed (Born-Oppenheimer approximation [6]). The molecule has two protons in which we consider their stationary positions. The electron that orbits around the protons has a certain probability in reference to its location. More simply, there is an explicit value that tells us the likelihood that the electron is in a specific location. We know from elementary physics that the electron is attracted to its opposite, the proton, hence the probability of the electron being closer to the protons will be much higher than when the electron is farther away. In order to compute this probability, we take the modulus of the wavefunction.

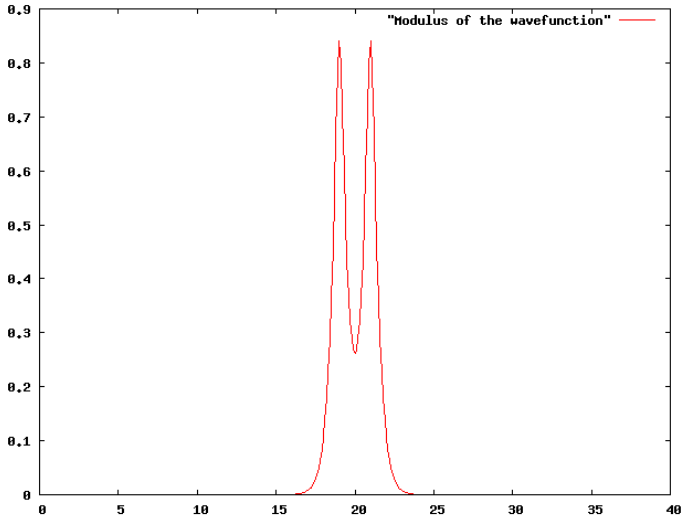

Figure 17: This figure illustrates the probability of precence of the electron for the H_2^+ molecule where the two nuclei are located at the two peaks of the graph

9 Conclusion

9.1 Results

We have demonstrated that through Gauge Theory, there are numerous different equations which can model the TDSE's. Firstly, we must select an appropriate Lagrangian which describes the dynamics of the system, followed by a corresponding Hamiltonian. Lastly, we select a gauge to represent the TDSE. Within this framework, we have explicitly chosen to work under the Coulomb Lagrangian, and the velocity and length gauges. Through careful calculations, we have seen that the physical observables of one gauge in comparison to another under the same Lagrangian can be obtained by a unitary transformation. Moreover, there exists motivations in selecting one gauge over another one. Specifically, the length gauge is simple however, it can become numerically inaccurate for very large domains. Although other numerical methods such as finite element methods are a possibility in order to approximate the TDSE, we choose to use a finite difference scheme to approximate ours. We have shown through numerical analysis that the scheme we have applied to approximate the velocity gauge is unconditionally stable, consistent and accurate to order 2 in time and space and convergent. Hence, we know that if we implement the model perfectly, that the finite difference scheme will result in a true solution. The model involves solving the Maxwell and Schrödinger equations in two different grids: Maxwell is at the macroscopic level and Schrödinger is at the microscopic level coupling with the polarization. The finite difference scheme results in a linear system of equations that needs to be solved where our matrix is a block matrix in which each of the blocks are tridiagonal matrices.
The numerical simulations have shown us that the length and velocity gauge produce the same results which is consistent with the Gauge theory analysis. Moreover, we illustrate the important physical observables such as the harmonics spectrum, incoming and outgoing electric field and lastly the probability of the electrons precence. The comparison between the length and velocity gauge has shown the same results when under the same initial conditions which is precisely the outcome we expect and desire.

9.2 Future Work

Potential further studies on this research can lead to many directions and paths. It would be interesting to implement the space translation gauge as theory entails that is equivalent to the length and velocity gauges. Although, it is more complex since it involves a moving mesh, this movement

of the mesh potentially will lead to a more accurate solution.
Furthermore, I would be highly motivated to employ a gauge from the Lorentz or Poincaré gauge. Although the Coulomb gauge field is the common gauge to solve the system, it would be fascinating to see how accurate the Lorentz gauge field is in comparison. From theory, we would expect them to produce consistent results, however perhaps one gauge field will lead to improved results due to mathematical and numerical reasons.

References

[1] O. Atabek, R. Lefebvre, and T. T. Nguyen-Dang. *Theory of intense laser-induced molecular dissociation: From simulation to control*, volume 10 of *Handbook of Numerical Analysis*. 2003.

[2] A. D. Bandrauk and H. . Lu. *Numerical methods for molecular time-dependent schrödinger equations - bridging the perturbative to nonperturbative regime*, volume 10 of *Handbook of Numerical Analysis*. 2003.

[3] Claude Cohen-Tannoudji, Jaques Dupont-Roc, and Gilbert Grynberg. *Photons and Atoms: Introduction to Quantum Electrodynamics*, chapter 1. Wiley, New York, Chichester, Brisbane, Toronto, Singapore, 1989.

[4] E. Lorin and A. Bandrauk. A simple and accurate mixed p0-q1 solver for the maxwelldirac equations. *Nonlinear Analysis: Real World Applications*, 12(1):190–202, 2011.

[5] E. Lorin and A. D. Bandrauk. *A Maxwell-Schrödinger-plasma model and computing aspects for intense, high frequency and ultrashort laser-gas interaction*, volume 5976 LNCS of *Lecture Notes in Computer Science (including subseries Lecture Notes in Artificial Intelligence and Lecture Notes in Bioinformatics)*. 2010.

[6] E. Lorin, S. Chelkowski, and A. Bandrauk. A numerical maxwell-schrödinger model for intense laser-matter interaction and propagation. *Computer Physics Communications*, 177(12):908–932, 2007.

[7] E. Lorin, S. Chelkowski, and A. D. Bandrauk. Mathematical modeling of boundary conditions for laser-molecule time-dependent schrödinger equations and some aspects of their numerical computation - one-dimensional case. *Numerical Methods for Partial Differential Equations*, 25(1):110–136, 2009.

[8] E. Lorin, S. Chelkowski, and A. D. Bandrauk. The wasp model: A micro-macro system of wave-schrödinger-plasma equations for filamentation. *Communications in Computational Physics*, 9(2):406–440, 2011.

[9] John C. Strikwerda. *Finite difference schemes and partial differential equations*. Wadsworth Publ. Co., Belmont, CA, USA, 1989.